Thomas Gamse, Amra Perva-Uzunalic (eds.)

Book of Abstracts

ESS-HPT 2018

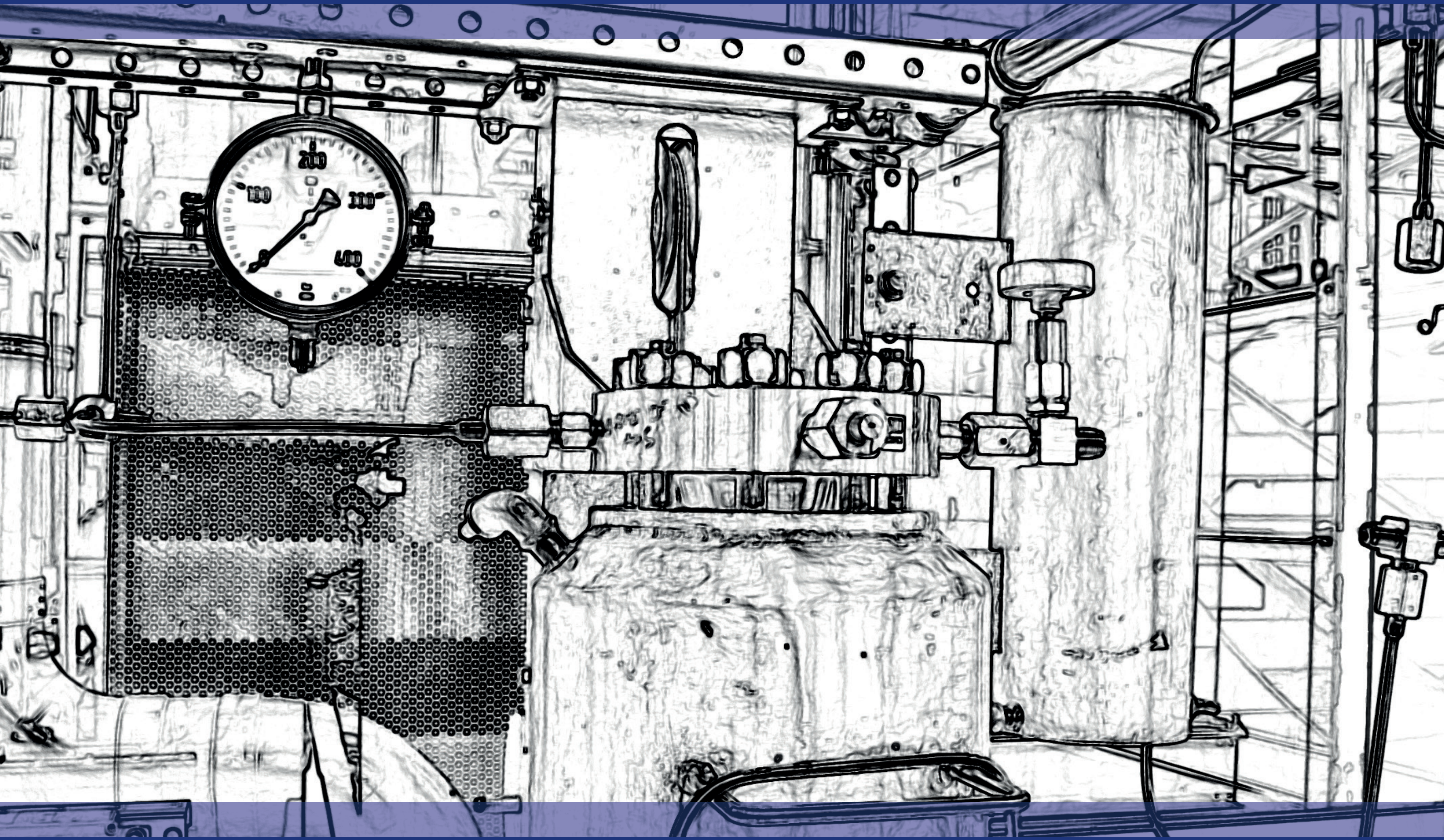

The European Summer School in High Pressure Technology

08.07. - 22.07.2018

TU Graz
Graz University of Technology

ICVT
pioneering the future

University of Maribor
Faculty of Chemistry and Chemical Engineering

EFCE
European Federation of Chemical Engineering
Europäische Föderation für Chemie-Ingenieur-Wesen
Fédération Européenne de Génie Chimique

Imprint

Organisation: Thomas Gamse
Institute of Chemical Engineering and Environmental Technology
Central Lab Biobased Products
Graz University of Technology, Inffeldgasse 25/C, 8010 Graz, Austria
Tel. +43 (0)316 873-7477
E-mail: thomas.gamse@tugraz.at

Zeljko Knez
Amra Perva-Uzunalić
Faculty of Chemistry and Chemical Engineering
Laboratory for Separation Processes
University of Maribor, Smetanova ulica 17, 2000 Maribor, Slovenia
E-mail: zeljko.knez@um.si; amra.uzunalic@um.si

Editor: Thomas Games, Amra Perva-Uzunalić
Layout: Thomas Games, Stefan Schleich
Cover: Thomas Games, Stefan Schleich

Book of Abstracts, ESS-HPT 2018,
The European Summer School in High Pressure Technology
8.7.-22.7.2018, University of Maribor and Graz University of Technology

ISBN (e-book) 978-3-85125-619-2

DOI 10.3217/978-3-85125-619-2

Preface

The European Summer School in High Pressure Technology (ESS-HPT) is the continuation of many years of high pressure intensive courses. The history of this very successful series of courses started in 1995, when the first intensive course took place in Monselice, Italy. Most of these Intensive Courses were supported by SOCRATES and later Life Long Learning, as shown in following overview:

SOCRATES IP "Current Trends in High Pressure Technology and Chemical Engineering"
1995 Monselice / Italy
1996 Nancy / France
1997 Erlangen / Germany

SOCRATES IP "High Pressure Technology in Process and Chemical Engineering"
1999 Abano Terme / Italy
2000 Valladolid / Spain
2001 Maribor / Slovenia and Graz / Austria

SOCRATES IP "High Pressure Chemical Engineering Processes: Basics and Applications"
2002 Graz / Austria and Maribor / Slovenia
2003 Budapest / Hungary
2004 Barcelona / Spain

SOCRATES IP "Basics, Developments, Research and Industrial Applications in High Pressure Chemical Engineering Processes"
2005 Prague / Czech Republic
2006 Lisbon / Portugal
2007 Albi / France

Life Long Learning IP "SCF- GSCE: Supercritical Fluids – Green Solvents in Chemical Engineering"
2008 Thessaloniki / Greece
2009 Istanbul / Turkey
2010 Budapest / Hungary

EFCE Intensive Course "High Pressure Technology - From Basics to Industrial Applications"
2011 Belgrade / Serbia

Life Long Learning IP "PIHPT: Process Intensification by High Pressure Technologies – Actual Strategies for Energy and Resources Conservation"
2012 Maribor / Slovenia and Graz / Austria
2013 Darmstadt / Germany
2014 Glasgow / Great Britain

Unfortunately the financial support for these Intensive Programmes was cancelled within ERASMUS+. The EFCE Working Party "High Pressure Technology" decided in September 2014 to go on with this course in the form of a Summer School.

ESS-HPT "The European Summer School in High Pressure Technology"

ESS-HPT 2015	Maribor / Slovenia and Graz / Austria
ESS-HPT 2016	Maribor / Slovenia and Graz / Austria
ESS-HPT 2017	Maribor / Slovenia and Graz / Austria
ESS-HPT 2018	Maribor / Slovenia and Graz / Austria

The ESS-HPT will take place every year within the first 2 weeks of July at University of Maribor, Slovenia and Graz University of Technology, Austria.

All participants have to give an oral presentation and the abstracts of these presentations, which are peer-reviewed by the EFCE WP Members, are published in this book of abstracts.

The editor

Thomas Gamse
Organiser of ESS-HPT 2018

Many thanks to our sponsors, NATEX Prozesstechnologie GesmbH and Tourismusverband Stadt Graz,

Contents

Abstracts of Participants Presentations

Wednesday, 11 July 2018 Night session

Thursday, 12 July 2018 Night session

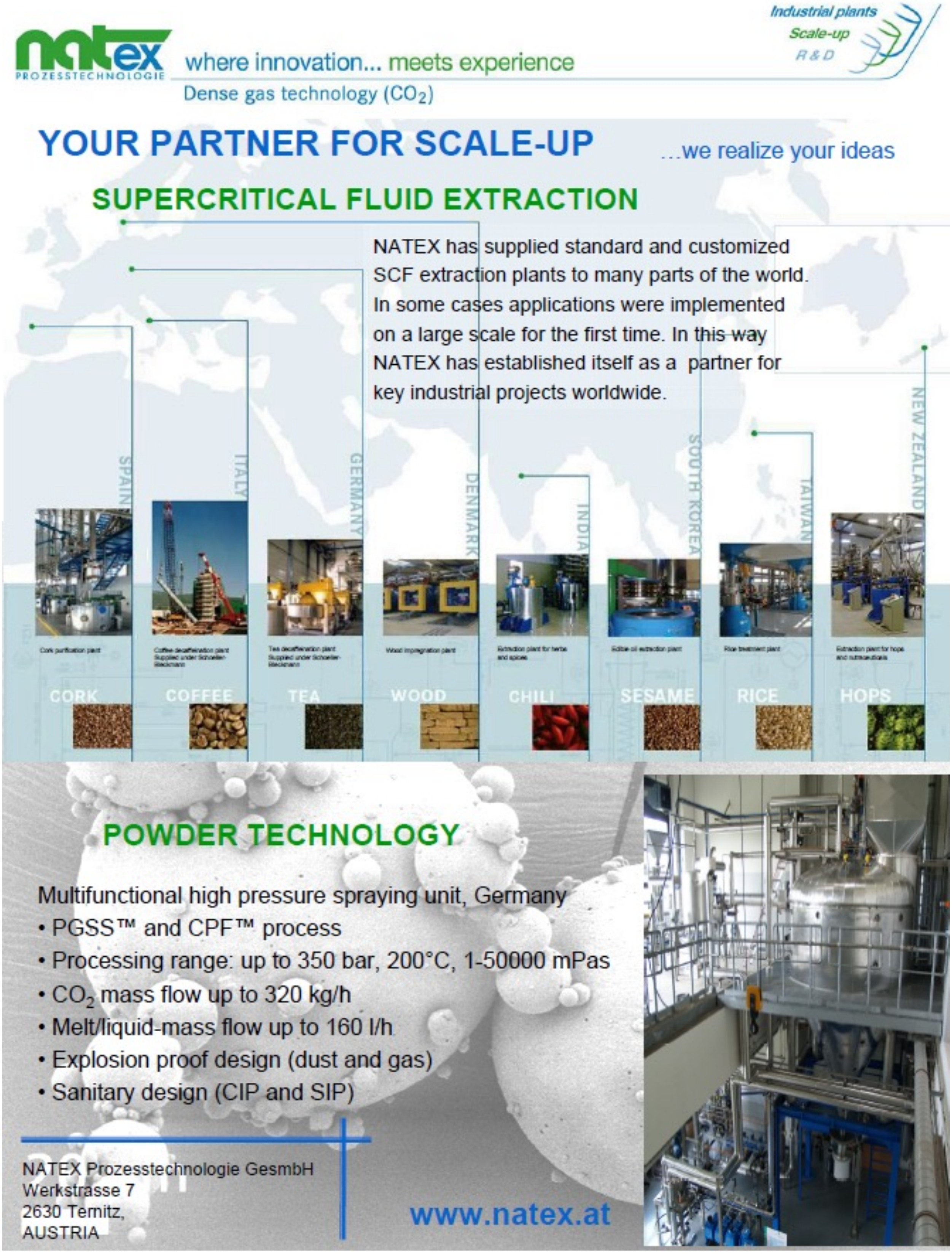

Non-Newtonian flow in porous media

Vincent Bürk

Chair of Particle Technology, Ruhr-University Bochum, buerk@fvt.rub.de

Introduction

To cover the increasing need for energy and oil for polymer production it is necessary to acquire new oil reserves. One potential solution is the heavy oil extraction through tertiary oil production methodologies like viscosity reduction due to gas solvation.

Through the shear thinning behaviour of the highly viscous heavy oil, unlike the Newtonian crude oil, the influence of gas solvation and shear rate on the viscosity becomes a point of focus. While the flow in pipelines can be described easily with only the shear viscosity as unknown variable, the flow of non-Newtonian fluids with a gas fraction in heterogeneous porous media is far more complex.

The aim of this work is to develop an experimental method to determine the shear rate dependent viscosity at reservoir conditions and to develop an empirical equation for the flow in porous media.

Experimental

The determination of the non-Newtonian flow is approached by using a high-pressure capillary rheometer as well as a permeameter including a hassler cell. The flow of non-Newtonian fluids in a heterogeneous porous medium is reliant on the geometrical properties of the porous medium as well as the rheological properties in dependency of the temperature, pressure, gas fraction and volume flow. The determination of the rheological properties of the homogenous fluid phase is approached by using a high-pressure capillary rheometer. The self-built capillary rheometer, shown in Fig.1, is designed for a pressure range from 0.1 MPa to 30 MPa and a temperature range from 293.15 K to 373.15 K. By varying the volume flow and the capillary diameter, shear rates up to 40000 1/s can be obtained. The set-up of the apparatus is described in [1] and the calibration procedure in [2].

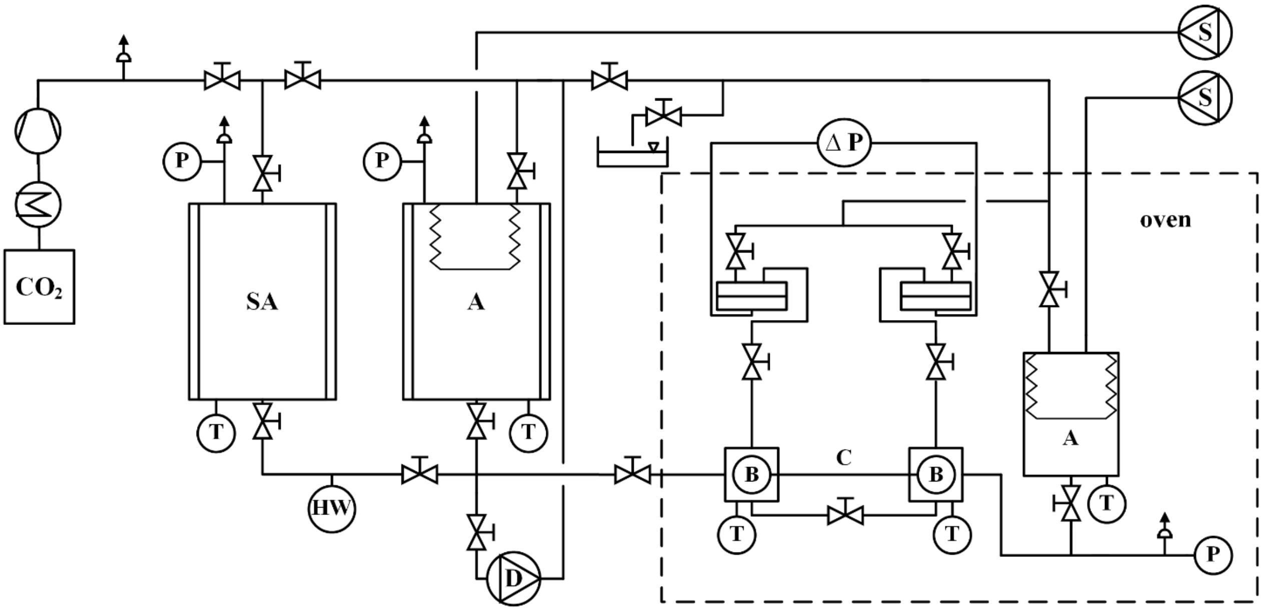

Fig. 1: Schematic principle of the capillary viscometer and the gas saturation section: (A) autoclave, (SA) saturation autoclave, (B) connection block, (C) capillary, (D) piston pump, (S) spindle press, (T) temperature sensor, (HW) heating wire, (P) pressure sensor, and (ΔP) differential pressure sensor.

Once the determination of the dynamic viscosity in dependency of the pressure, temperature, shear rate and gas solvation is completed, the properties of the heterogeneous porous medium need to be acquired.

The porous media used, consists of homogeneous, artificially made capillary bundles and glass beds as well as heterogeneous sandstone cores drilled out of Berea- and Bad Bentheim sandstone. After crafting the porous samples, the geometrical properties like length, diameter as well as absolute and effective porosity have to be measured. Subsequently the permeability of the samples can be obtained by using a permeameter including a Hassler-cell shown in Fig.2.

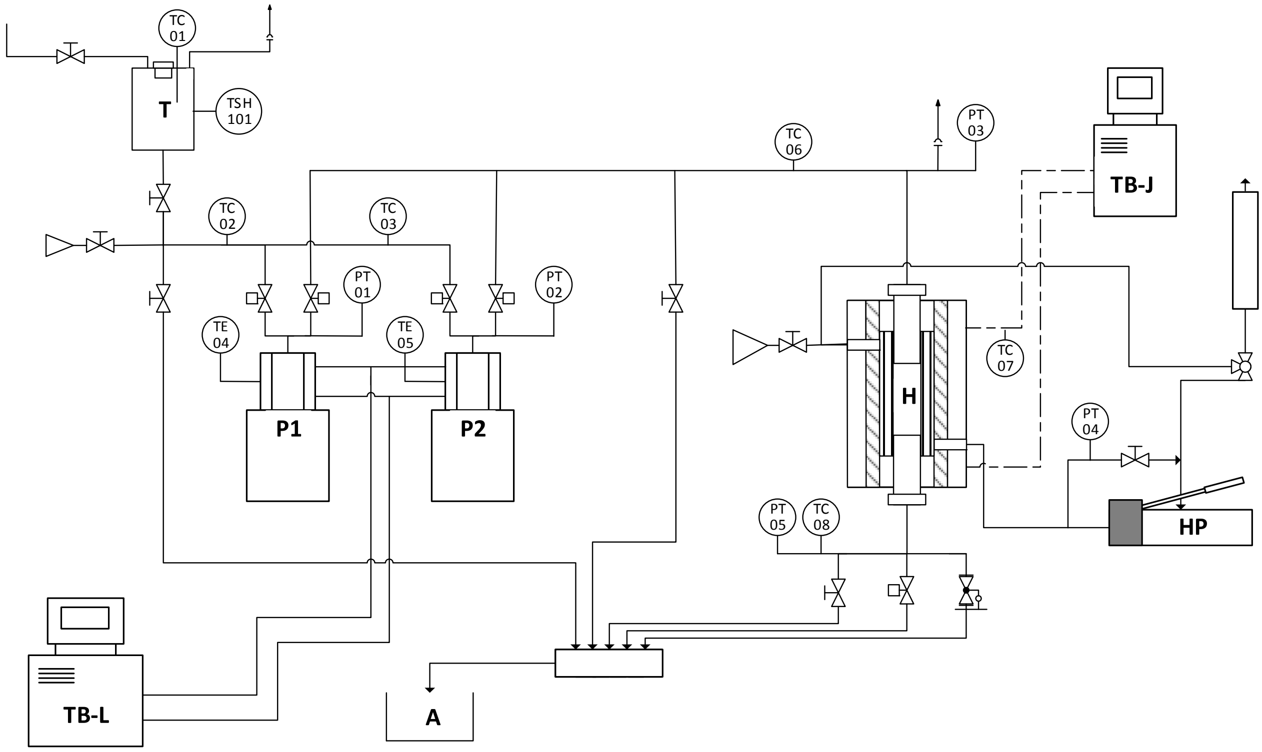

Fig. 2: Schematic principle of the permeameter including a Hassler-Cell

The permeameter is designed for permeability measurements of core samples with a diameter of 40 mm and lengths from 50 mm up to 200 mm. After inserting the sample into a Viton sleeve fitted in a Hassler-Cell, it can be flushed with pressures up to 60 MPa and volume flows from 0.1 ml/min up to 20 ml/min. By using a Newtonian fluid, like water, the differential pressure over a core sample with a constant volume flow is measured and thus the permeability of the sample can be calculated with Darcy´s law.

$$K = \frac{Q \cdot \eta \cdot L}{A \cdot \Delta p} \qquad \text{Eq.1}$$

After determining the properties of the porous medium with a Newtonian fluid, the sample is dried and the pressure loss in dependency of the volume flow is again measured in the Hassler-Cell with the previously measured non-Newtonian fluid. Through the combination of all measurements, it is possible to gain knowledge about the flow of the non-Newtonian fluid in the porous medium.

Summary

In the progress of this work viscosity measurements of non-Newtonian, Newtonian, and Newtonian fluids with gas solvation have been made. Through the gained experience several liquids have been chosen for the studies within porous media. Due to the complex flow in the heterogeneous structure of sand stone core samples, artificial porous media has been constructed and tested to gain information about the flow. As soon as an equation for the determination of the shear in the artificially made porous media has been found which is comparable to the measured shear rate, further measurements with the drilled sand stone cores and heavy oil like substances will be carried out.

References

[1] S. Hüttemann, S. Pollak, S. E. Quiñones-Cisneros, E. Weidner, Development of a Capillary Rheometer for the Characterization of Heavy and Extra-Heavy Oils, Energy Fuels 29 (5), S. 2876–2882. DOI: 10.1021/ef5020988.

[2] J. Kremer, V. Bürk, S. Pollak, A. Kilzer, M. Petermann, Viscosity of squalane under carbon dioxide pressure - Comparison of acoustic levitation with conventional methods, The Journal of Supercritical Fluids,

https://doi.org/10.1016/j.supflu.2018.02.007

Selectivity of analytical extraction and chromatography methods for phenolic compounds from Morupule coal and coal tar

Fiona Maungo Nermark, Department Of Chemistry, Lund University, Sweden,
fiona_maungo.nermark@chem.lu.se
and
Nanomaterials, Botswana Institute for Technology Research and Innovation, Botswana

Introduction

Coal is described as a sedimentary rock. Coal is formed from dead plant matter that was converted into peat, which in turn is converted into lignite, then sub-bituminous coal, after that bituminous coal, and lastly anthracite. This involved biological and geological processes over billions of years ago. Coal also contains mineral matter that is thought to have been deposited into the coal pits from surrounding rocks by water. Coal is extracted from the ground by either underground mining or open pit mining. Coal properties depend mainly on its age, vegetation that it was formed from and the minerals present. Therefore, it is very important that it is characterized before utilization[1].

Coal has many important uses worldwide. The most significant uses of coal are in electricity generation, steel production, cement manufacturing and as a liquid fuel[2]. Other important users of coal include alumina refineries, paper manufacturers, and the chemical and pharmaceutical industries. Several chemical products can be produced from the by-products of coal. Refined coal tar is used in the manufacture of chemicals, such as creosote oil, naphthalene, phenol, and benzene. Ammonia gas recovered from coke ovens is used to manufacture ammonia salts, nitric acid and agricultural fertilizers[3].

Botswana's coal deposit forms part of the Karoo Supergroup[4]. Currently, Morupule Coal Mine (MCM) is the only active mine. The MCM coal is part of the eastern margin of the South East Central Kalahari Karoo Sub Basin. The coal is overlaid by shale, sandstones, mudstone and siltstone[4]. The total cumulative thickness of the seams is 22 to 25 m. The total in-situ coal resources is approximately 4 billion tons.

The relevance of the project is based on coal beneficiation, beyond electricity generation. This projects seeks to come up with methods that can be used to extract high value chemicals such as phenolic compounds from Morupule coal. Phenolic compounds with application as starting material in the synthesis of industrial organic chemicals[5].

Pressurized hot water extraction and supercritical fluid extraction are the two extraction methods that are attractive because they use very little organic solvents and sometimes surfactants as modifiers, or no organic solvents still achieving short extraction times[6,7]. During this project, the above mentioned methods will be extensively explored because they are environmentally friendly.

The main aim of this thesis is to explore the selectivity of supercritical carbon dioxide (SC-CO_2) and Pressurized hot water extraction (PHWE) for the extraction and analysis of phenolic compounds from raw coal and coal tar. The research questions are; firstly, what are the physical characteristics of the coal (the sample matrix), how does heat (TGA) affect the coal, which compounds (or compound classes) are extractable using SC-CO_2 and PHWE with the focus. The main focus will be identification and quantification of phenolic compounds from the extracts.

Experimental

The coal will first be characterized through proximate and ultimate analysis of the coal, the calorific value of the coal and mineral composition of the coal following American Society for Testing and Materials (ASTM) standard method. This data will give the coal ranking. The methods that will be used are elemental analysis, thermogravimetric analysis, calorimetric analysis and X-Ray Fluorescence Spectroscopy.

Pyrolysis, PHWE and SC-CO_2 extraction experiments will be done by employing response surface methodology (RSM). The influence of independent variables, such as pyrolytic temperature, heating rate, catalyst for pyrolysis experiments and solvents, extraction temperature, time, as well as solvent-to-sample ratio for PHWE and SC-CO_2 on response variables will be explored.

Analysis of PHWE and SC-CO_2 extracts will be carried out using a range of different separation methods based on Gas Chromatography/Mass Spectrometry (GC/MS) and Ultra Liquid Performance –Quadrupole Time of Flight/Mass Spectrometry (UPLC-QToF/MS).

Acknowledgment

Acknowledgement is made to the Green Technology Group in the Centre for Analysis and Synthesis (CAS) at Lund University, Sweden and Botswana Institute for Technology, Research and Innovation (BITRI) for funding. Morupule coal mine for the coal samples.

References

(1) Speight, J. G. *Chemistry and technology of coal*, 3rd ed.; CRC Press: [Place of publication not identified], 2016; pp 14-18.

(2) Han, L.; Zhang, R.; Bi, J.; Cheng, L. *J. Anal. Appl. Pyrolysis* **2011**, *91* (2), 281–287.

(3) Xie, K.; Li, W.; Zhao, W. *Energy* **2010**, *35* (11), 4349–4355.

(4) Cairncross, B. *J. African Earth Sci.* **2001**, *33* (3), 529–562.

(5) Grand View Research Inc. Global Phenolic Resins Market Size | Industry Research Report, 2025 https://www.grandviewresearch.com/industry-analysis/phenolic-resins-market (accessed May 13, 2018).

(6) Mustapa, A. N.; Manan, Z. A.; Azizi, C. . Y. M. *J. o/Chemical Nat. Resour. Eng.* 164–180.

(7) Machado, B. A. S.; Pereira, C. G.; Nunes, S. B.; Padilha, F. F.; Umsza-Guez, M. A. *Sep. Sci. Technol.* **2013**, *48* (18), 2741–2760.

High Pressure Ethene Homo-/Copolymerization on Mini-Plant Scale

C. Mohl, M. Busch

Ernst-Berl-Institut/ Technical Chemistry III,Technische Universität Darmstadt,
markus.busch@pre.tu-darmstadt.de

LDPE is produced by free radical polymerization under high pressure and temperature (1000 to 3000 bar, >200 °C). It has a contend of 18% of the European plastics converter (2016) with an important role in today’s polyolefin industry.[1] To vary the material properties, it can be copolymerized with different comonomers. Due to the extreme conditions, only a few research groups investigate the polymerization process on mini-plant scale. The group of *M. Busch* develop different mini plant systems based on the work of *G. Luft* & *M. Buback*, to produce LDPE in batch and continuous processes.

For small sample amounts (0,5 g to 2 g), a 30 mL batch autoclave including an injection system is used. The autoclave is designed for pressures up to 3000 bar and temperatures of 300 °C. An exploded assembly drawing of the reactor is shown in figure 1. With two sapphire-windows it is possible to look inside the reactor during experiments. A high-speed camera allows recording the insight of the autoclave with 200 fps. To bring substances like initiators or comonomers inside the reactor during an experiment a Micro-Injection-System is included. The system consists of a pneumatic valve, which is controlled with a Programmable Logic Controller (PLC) and an injection line with a changeable volume of actual 0.6 mL. With a higher pressure on the injection line, substance can be injected nearly deadvolume free into the reactor.

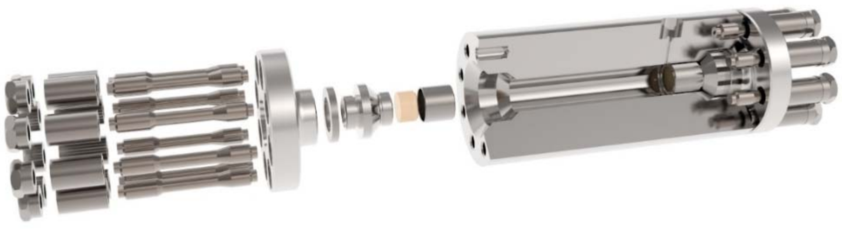

Figure 1: Exploded assembly drawing of the 30 mL reactor.

For higher sample amounts, the mini-plant is used. The experiments can be carried out in batch ore continuous mode. The mini-plant is equipped, which a 100 mL autoclave witch offers reaction conditions up to 3000 bar and 300 °C. The assembled autoclave with mounted stirrer is depicted in figure 2.

Figure 2: Assembled 100 mL autoclave with stirrer.

To dosage comonomer, initiators ore other substances there are three systems with different flow ranges. For small feeds two syringe pumps used for a range of 2 mL/h to 4 mL/h. The first syringe is a *Nova Swiss* 10 mL, the second one an in-house built 20 mL. High feed rates are realised with three *Orlita* membrane pumps for a range of 80 g/h to 1 kg/h each. An in house build volume changer with a range of 5 mL/h to 55 mL/h closes the gap between the pumps and the syringes. All feed streams get together with the ethene through the stirrer aggregate into the reactor.

The ethene gets compressed to reaction conditions with one of three compressors. A 2000 bar *Hofer* membrane-, a 3000 bar Hofer membrane- and a 3000 bar *Hofer* dry running piston-compressor. The feed rate of ethene is set to 26.4 NL/h wherby the residence time in the autoclave is 90 s. Next to the mentioned dosing systems liquid gases can be fed directly into the 3rd stage of the 3000 bar membrane compressor. If oxygen is used as an initiator, it can be fed into the ethene line before the 3000 bar membrane compressor.

In summary, the 30 mL reactor setup can be used for experiments on a minor time scale with limited possibilities of dosing substances, whereas the mini-plant with the 100 mL reactor is flexible of dosing different substances.

References

[1] https://www.plasticseurope.org/de, *Plastics the facts 2017*, June 10th **2018**

Towards general optimization of electrochromic cells and other optoelectronic devices

Martin Rozman, Martin Gladović, Urban Bren
Faculty of chemistry and chemical technology, University of Maribor
martin.rozman1@um.si

Introduction

Optoelectronics is the study of electronic devices and systems that can transform electric signals into light response or vice versa. For instance, electrochemical devices possessing capability of reversible colour change under applied electric potential, while maintaining stable colour after the potential has been turned off, are known as electrochromic devices (ECDs). Multiple types of these devices exist, that use different electrochromic materials [1], and can use different types of electrodes, such as thin film metal deposit, transparent conductive oxides, or transparent conductive polymers. These conductive polymers such as polyethylenedioxythiophene (PEDOT) or PEDOT-PSS are invaluable in optoelectronic research since they are often the main material from which optically transparent electrodes (OTE) are made. Polymers can be prepared in different ways, but in recent years supercritical CO_2 drying has been shown as the most promising candidate to be used in large industrial scales [2].

Chemical reactions in some electrochemical devices can also be influenced by external factors. Typical representatives of such systems are dye-sensitized solar cells (DSSCs) which can be basically classified as photoelectrochemical cells. In these cells, the incident solar light is used as the energy that drives chemical reaction used as a source of electric energy. The discovery that TiO_2 applied on a transparent conductor can act as a photoactive electrode further boosted the development of DSSCs [3]. Both ECDs and DSSCs usually consist of at least one optically transparent electrode (OTE), counter-electrode, electroactive dye and electrolyte [4].

In the past decade the optoelectronic research focused mostly on less expensive materials to develop new types of devices with more efficient mechanisms, where for example, in photovoltaic field DSSCs were surpassed by more efficient perovskite solar cells, while in the field of electrochromics no major advances were made after the development of WO3-type electrochromic cells.

Experimental

An electrochromic cell that uses thin nanocrystalline TiO_2 films coated on electrodes and has adsorbed Fe(II) and Co(II) bipyridine complexes was initially investigated [5]. The operation of the cells was analysed using cyclic voltammetry as well as by UV-Vis reflectance and transmittance spectroscopy.

The next investigated system was an electrochromic cell, which uses electrodeposition of lead (II) oxide in combination with hydrogel stabilized water-based electrolyte. Hydrogel polymer was prepared using free radical polimerization technique and was freeze dried before it was used in combination with water electrolyte [6]. Operation of selected devices was examined using a series of electrochemical techniques (cyclic voltammetry, chronoamperometry, and electrochemical impedance spectroscopy), along with UV-Vis transmittance spectroscopy.

In addition, already known electrochromic and photovoltaic systems were investigated regarding how well they behave if they are assembled in different geometrical configuration, using no OTE. Fluorine doped tin oxide (FTO) in Vincent device [7] was removed and stainless steel electrodes were positioned in back-to-back configuration to form a non-transparent ECD that used pH dependant dye for its mode of operation. The constructed device was again investigated using different electrochemical techniques such as cyclic voltammetry and chronoamperometry along with UV-Vis reflectance spectroscopy.

A photovoltaic device was also constructed in a similar configuration, where FTO was also replaced with stainless steel foil, while the rest of the device was left unchanged. Device was then characterized using solar simulator and cyclic voltammetry.

Summary

An ECD that uses TiO_2 films with adsorbed Co or Fe dyes had coloration response times in order of one second, while the difference between both colored states was clearly visible. Best characteristics were obtained with the cobalt bipyridine hexafluorophosphate complex dye adsorbed on a mesoporous TiO_2 electrode in combination with NiO counter-electrode. Devices created according to the described method could potentially be used to recycle and re-use exhausted dye-sensitized solar cells for transparent smart windows, or as a new type of displays.

Another ECD that used electrodeposition of PbO had relatively slow response times, however it showed excellent transmittance differential of 20% between bleached and tinted state, stable colour in both states and the ability to self-bleach when short-circuited. This type of electrochromic cells could be used as a more durable and lower cost replacement for existing intercalation-type electrochromic devices.

Fig 1: ECD that uses electrodeposition of PbO in bleached (left) and tinted (right) state

ECDs, with pH dependant dye, that use a different geometrical approach and were constructed without OTE behaved very similar to original Vincent devices with similar response times and identical colour response.

Photovoltaic devices that used a different geometric approach achieved slightly lower potential and lower current than their original counterparts; however they demonstrated that it is possible to construct an inexpensive photodiode without OTE.

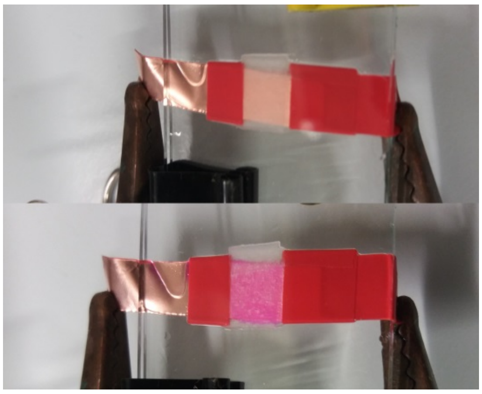

Fig 2: ECD that uses pH dye phenolphtalein in bleached (top) and tinted (bottom) state

Acknowledgments

I would like to thank the financial support through Slovenian Research Agency project grant J1-6736 and Slovenian Ministry of Education, Science and Sports program grant F4F. Additionally I would like to thank Dr. U. Bren, Dr. R. F. Godec, Dr. M Lukšič and and Dr. E. Stathatos for improving my knowledge on general electrochemistry, optoelectronics and materials science.

1. Patel, K.J., et al., *All-inorganic solid-state electrochromic devices: a review.* Journal of Solid State Electrochemistry, 2017. **21**(2): p. 337-347.
2. Zhang, X., et al., *Conducting polymer aerogels from supercritical CO2 drying PEDOT-PSS hydrogels.* Journal of Materials Chemistry, 2010. **20**(24): p. 5080-5085.
3. O'Regan, B. and M. Gratzel, *A low-cost, high-efficiency solar cell based on dye-sensitized colloidal TiO2 films.* Nature, 1991. **353**(6346): p. 737-740.
4. *Fundamentals of device construction*, in *Electrochromism and Electrochromic Devices*, D. Rosseinsky, P. Monk, and R. Mortimer, Editors. 2007, Cambridge University Press: Cambridge. p. 417-432.
5. Rozman, M., et al., *Electrochromic properties of thin nanocrystalline TiO2 films coated electrodes with adsorbed Co(II) or Fe(II) 2,2'-bipyridine complexes.* Electrochimica Acta, 2017. **238**: p. 278-287.
6. Konstantinos, P. and B. Georgios, *Simultaneous lower and upper critical solution temperature-type co-nonsolvency behaviour exhibited in water–dioxane mixtures by linear copolymers and hydrogels containing N-isopropylacrylamide and N,N-dimethylacrylamide.* Polymer International, 2006. **55**(11): p. 1254-1258.
7. Vincent, J.B. and D.W. Flick, Vincent, J. B.; Flick, D. W., Electrochromic display device: *patent US 7054050 B2*: **2006**.

Development and Optimization of Supercritical Water Desalination (SCWD) Unit

Surika van Wyk

Sustainable Process Technology – Faculty of Science and Technology, University of Twente , s.vanwyk@utwente.nl.

Introduction

In the past 20 years the global desalination capacity has increased with 58 million m^3/d, with the capacity being 86.6 million m^3/d in 2015 [1]. Desalination technologies are not only limited to seawater purification, but are also used to treat brackish water, river water, wastewater and brine. The purified water is used in numerous sectors including various industrial applications, power stations and tourism with municipal applications being the majority user. Conventional desalination technologies include reverse osmosis (RO), multi-stage flash distillation (MSF), multiple-effect evaporation (MEE) and electrodialysis, with RO and MSF being the most used technologies [2]. Even though these technologies are well established, there are certain drawbacks such as low water recovery, of ± 45% for seawater RO [3] and ± 50% for thermal processes such as MSF and MEE [4]. Parallel to the production of freshwater, these processes also generate brackish waste streams, which need to be managed. One of the major problems with the treatment of the brine is the disposal into the oceans by coastal plants, which disrupts the marine ecosystems [3]. In recent years more stringent regulations have been put into effect for discharging the brines for conventional desalination processes and waste streams from hydraulic fracturing and for this reason zero liquid discharge (ZLD) technologies have been investigated and further developed [5–7]. ZLD technologies provide a manner to eliminate the production of brine streams, thereby reducing the impact of desalination on the environment. Supercritical water desalination (SCWD) is a novel technology, that separates inorganic compounds from brackish water, with the potential of being a ZLD technology [8,9].

At supercritical conditions (Pressure > 22.5 MPa, Temperature > 374 °C) the properties of water start to change significantly. The density of water decreases, which reduces its polarity due to weaker hydrogen bond interactions. Consequently, the solubility of inorganic compounds decreases, resulting in the formation of solid salt in supercritical water [10]. The potential of SCWD was investigated earlier through phase equilibria experiments of NaCl-H_2O solutions on laboratory scale. The results were used to illustrate a proof-of-principle for a two-stage separation process [8]. The first stage of separation is the removal of supercritical water (SCW) from a liquid brine solution occurring in the vapour – liquid region at supercritical conditions (see Figure 1). The next stage is the separation (expansion) of the liquid brine into salt and steam at subcritical conditions.

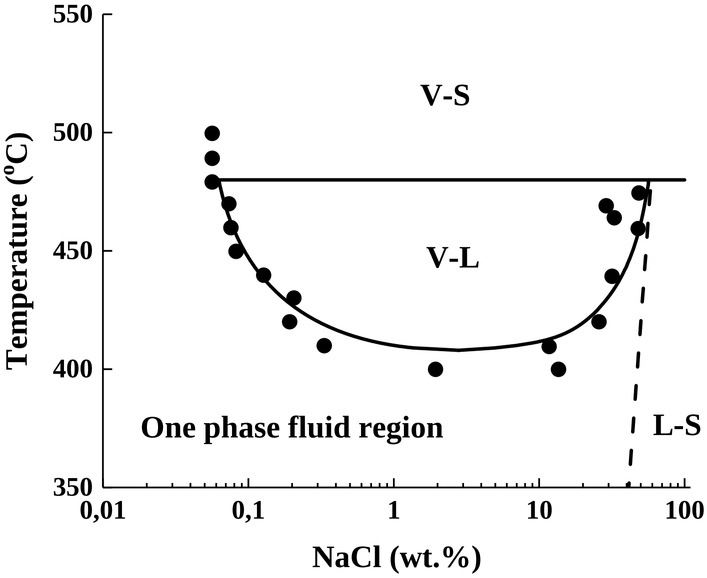

Fig 1: Phase diagram of NaCl-H_2O system at 300 bar (-Model, ● Experimental data) [9].

Based on the proof-of-principle study a pilot plant has been designed, constructed and tested [9]. Preliminary results have shown that SCWD technology is feasible, with calculations showing that ZLD is attainable. However, the systems need to be further developed to make it more energy efficient and economically feasible.

Experimental

A schematic of the SCWD pilot plant is shown in Figure 2. The pilot plant is divided into two stages. The first is a gravity separator in which SCW is continuously separated from a concentrated brine. The second stage is the rapid expansion of the concentrated brine into solid salt and steam (occurs at 1 bar and 100 °C). Experiments are done with (3 - 16 wt.%) NaCl-water solution, at 270 bar and 430 °C.

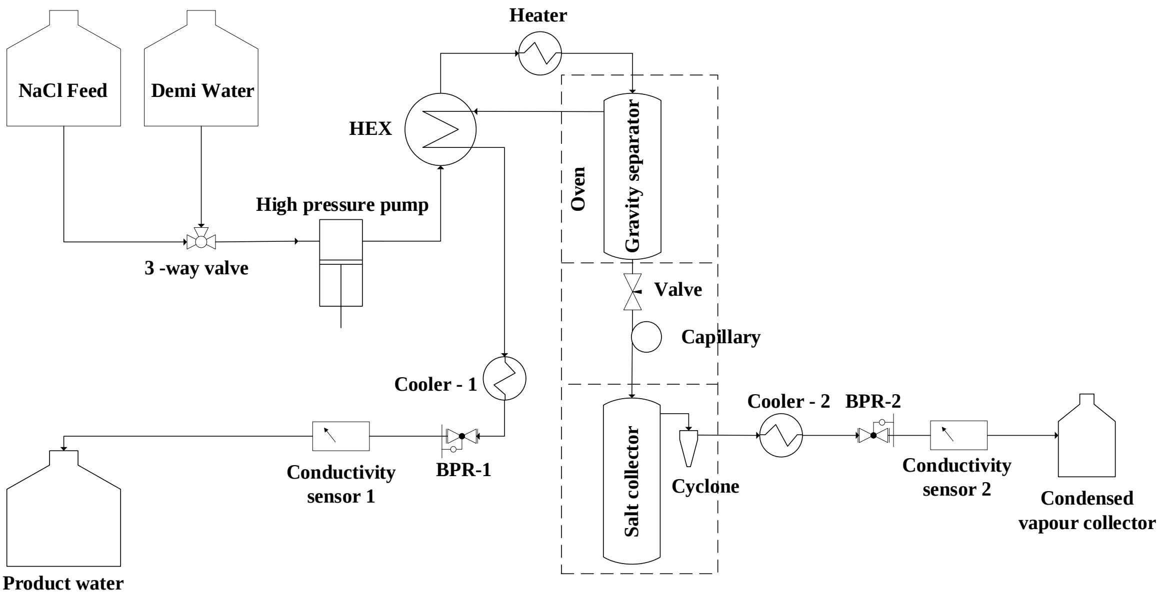

Fig 2: SCWD pilot plant layout [9]

First results of the plant showed that drinking water quality can be obtained, with a concentration of ± 600 ppm NaCl. For a feed concentration of 3.5 wt.% NaCl, the recovery of drinking water is ± 91%, similar to what is expected from thermodynamics.

Summary

The focus of the research is to further develop and optimize SCWD in terms of the energy consumption and the productivity. This is achieved by modelling the system thermodynamically, investigating the influence of other salts on the separation process *etc*. The goal is to develop a more continuous set-up that can be integrated with conventional desalination technologies in order to reduce overall energy consumption and to attain ZLD.

Acknowledgment

This work was performed in the cooperation framework of Wetsus, European Centre of Excellence for Sustainable Water Technology (www.wetsus.nl). Wetsus is co-funded by the Dutch Ministry of Economic Affairs and Ministry of Infrastructure and Environment, the European Union Regional Development Fund, the Province of Fryslân and the Northern Netherlands Provinces. This work is part of a project that has received funding from the European Union’s Horizon 2020 research and innovation program under the Marie Skłodowska-Curie grant agreement No 665874.

References

[1] IDA, Desalination by the Numbers, Int. Desalin. Assoc. (2017).

[2] D. Xevgenos, K. Moustakas, D. Malamis, M. Loizidou, An overview on desalination & sustainability: renewable energy-driven desalination and brine management, Desalin. Water Treat. 3994 (2014) 1–11. doi:10.1080/19443994.2014.984927.

[3] L.F. Greenlee, D.F. Lawler, B.D. Freeman, B. Marrot, P. Moulin, Reverse osmosis desalination: Water sources, technology, and today’s challenges, Water Res. 43 (2009) 2317–2348. doi:10.1016/j.watres.2009.03.010.

[4] J.E. Miller, Review of water resources and desalination techniques, Sand Rep. (2003) 1–54. doi:SAND 2003-0800.

[5] D. Xevgenos, K. Moustakas, D. Malamis, M. Loizidou, An overview on desalination & sustainability: renewable energy-driven desalination and brine management, Desalin. Water Treat. 57 (2016) 2304–2314. doi:10.1080/19443994.2014.984927.

[6] H.W. Chung, K.G. Nayar, J. Swaminathan, K.M. Chehayeb, J.H. Lienhard V, Thermodynamic analysis of brine management methods: Zero-discharge desalination and salinity-gradient power production, Desalination. 404 (2017) 291–303. doi:10.1016/j.desal.2016.11.022.

[7] D.D. Ogden, J.P. Trembly, Desalination of hypersaline brines via Joule-heating: Experimental investigations and comparison of results to existing models, Desalination. 424 (2017) 149–158. doi:10.1016/j.desal.2017.10.006.

[8] S.O. Odu, A.G.J. Van Der Ham, S. Metz, S.R.A. Kersten, Design of a Process for Supercritical Water Desalination with Zero Liquid Discharge, Ind. Eng. Chem. Res. 54 (2015) 5527–5535. doi:10.1021/acs.iecr.5b00826.

[9] S. van Wyk, S.O. Odu, A.G.J. van der Ham, S.R.A. Kersten, Design and results of a first generation pilot plant for supercritical water desalination (SCWD), Desalination. 439 (2018). doi:10.1016/j.desal.2018.03.028.

[10] F.J. Armellini, J.W. Tester, Solubility of sodium chloride and sulfate in sub- and supercritical water vapor from 450-550 C and 100-250 bar, Fluid Phase Equilib. 84 (1993) 123–142. doi:10.1016/0378-3812(93)85120-B.

Pressure Pulsations in Piping Systems under Pump Excitation

Michael Feist

Institute of Process Machinery and Systems Engineering, Friedrich Alexander University Erlangen-Nuremberg, fe@ipat.uni-erlangen.de

Introduction

Pressure pulsations in piping systems can cause serious damage to components in plants. One example is the water hammer effect that can result in heavy damages. Especially piston pumps can generate pressure waves with large amplitudes. To design hydraulic piping systems the 1-D method of characteristics is a useful method. It solves the 1-D flow equations and as a result, the user can interpret the calculated data like pressure or flow rate depending on the time. In this simulation, a piston pump is modelled as a pulse generator.

The current method of characteristics for flow elements has problems to calculate the oscillations generated by piston pumps. Target of this work is to improve the existing model and evaluate it with a test facility.

Experimental

Based on an existing test facility a new setup will be built to investigate the pressure wave propagation in piping systems.

On the pressure side, the length of the piping systems is 28 metres and the inner diameter of the pipe is 25 mm. To reduce structural oscillations the pipe system is fixed at a stiff structure. The system is running with a piston pump to generate the pressure oscillations. The pressure is measured at eight different points of the system. In addition, the piping system is modelled in a 1-D characteristics program to compare the tests with a simulation model. Based on the results of this comparison the existing simulation model can be improved and again be evaluated with the test facility. On the suction side of the pump, optical measurements are possible to study cavitation in the pipelines.

To create knowledge about pressure wave propagation into cavitation areas a separate test facility is planned. Furthermore basic investigations of pressure wave propagation in different single pipe segments like pipe bends, tee joints and more will be made.

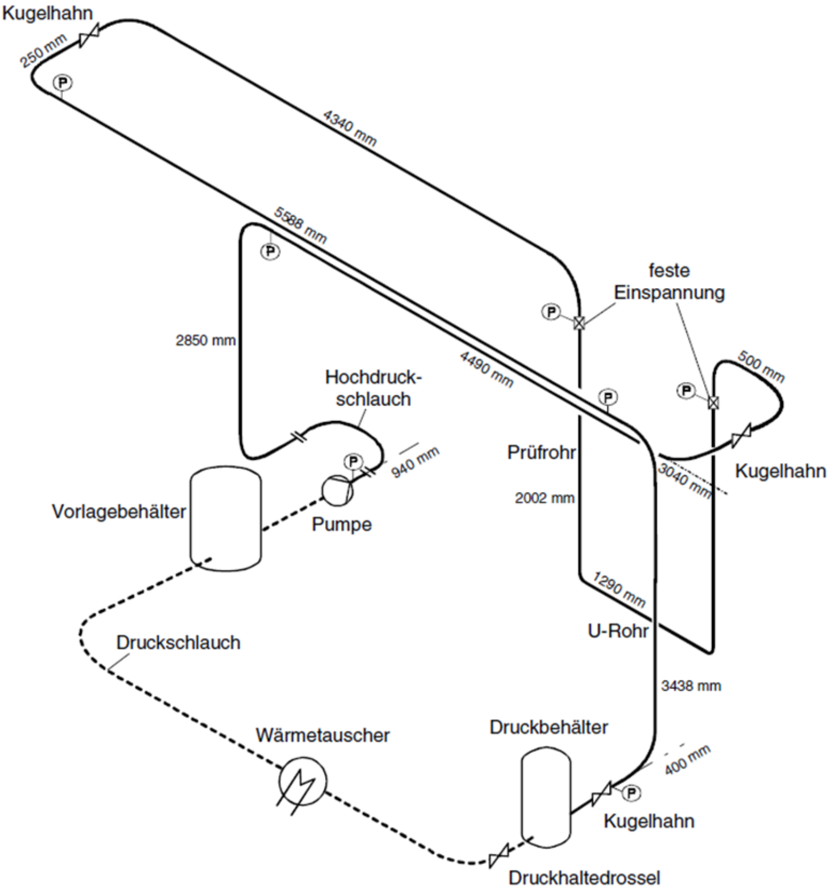

Fig. 1: Existing test facility

Summary

This work aims to develop a better simulation model for pressure waves in piping systems. With the combination of simulation and measurements, the complex field of pressure wave propagation in piping system can be researched.

References

[1] S. Riedelmeier, Quantification of fluid-structure interaction effects during water hammer in piping systems, Erlangen: Shaker Verlag, 2017.

[2] D. Jarmer, Zur Erregung mechanischer Rohrleitungsschwingungen durch oszillierende Verdrängerpumpen - Numerische Berechnung und experimentelle Verifikation-, Erlangen, 2002.

Stabilization of Amorphous Active Substances in Polymer-Based Formulations

Alberto Bueno Morales

Thermal Separation Processes, TUHH, alberto.bueno@tuhh.de

The pharmaceutical industry has made giant strides in the research and development of drugs and excipients aimed at treating infectious and deadly diseases. The stabilisation of amorphous solid forms is one of the most important strategies for increasing the bioavailability of modern, usually very lipophilic active substances (API). The bioavailability of the drug in the human body is improved when the drug is in amorphous form compared to crystalline form. However, state of the art methods can only process dosage forms containing the drugs in crystalline form on a commercial scale.

If an API is present in its metastable, amorphous form, there is a risk of recrystallisation during storage. This process can be avoided or delayed by using an auxiliary as a matrix. The API is either solubilised molecularly in the matrix or deposited in the pores of a porous matrix. The encapsulation of APIs in micro or mesoporous solid supports enables stabilisation of amorphous API forms. In recent years, highly porous, organic aerogels have been increasingly used for this purpose.

Organic polymers in the form of aerogels which contain a three dimensional structure network can be loaded with API´s up to 70%.

The goal of this project is a new one-pot approach towards a fast and efficient production of amorphous solid drug dosage forms with improved bioavailability. Also, the scaling up of the process is going to be considered. Considering the kinetics of solvent exchange under pressure and a thermodynamic approach to understanding the underlying principles of the solvent exchange, extraction and impregnation.

Towards Identification of Polyphenolic Scavengers of Chemical Carcinogens from Various Natural Sources – A Computational Aproach

Veronika Furlan, Martin Gladović, Urban Bren
Faculty of Chemistry and Chemical Technology, University of Maribor
veronika.furlan@um.si

Introduction

Natural dietary agents from different sources including fruits, vegetables, and spices have drawn a great deal of attention from both the scientific community and the general public due to their various health-promoting effects including cancer prevention. Polyphenols represent a large and diverse group of secondary plant metabolites and are therefore abundantly present in a majority of fruits, vegetables, spices and herbs. The protective role of polyphenols against reactive oxygen and nitrogen species, UV light, plant pathogens, parasites and predators results in several beneficial biological activities, which can provide an effective protection against or even cure of several prevailing diseases, including various types of cancer.[1] Cytoprotective effects toward normal cells and cytotoxic effects toward cancerous cells, high accessibility as well as low systemic toxicity represent the main advantages of polyphenols as anticarcinogenic agents.[2]

The main obstacle to utilize polyphenols as chemopreventive agents lies in their limited bioavailability and rapid metabolism. However, there are several ways to improve the absorption or to reach the desired effect at lower doses. The most promising solution to avoid the degradation and improve the absorption of polyphenols is nanoencapsulation.[1] Several encapsulation techniques (spray drying, spray chilling and cooling, coacervation, fluidized bed coating, liposome entrapment) have been used to convert liquid components into solid particles and to provide their controlled release.[3] Another possible solution is the use of mixtures of several biologically active polyphenols that bring synergistic effects and significantly reduce dose-related toxicity. The combination of polyphenols with existing anti-cancer drugs and therapies can also achieve the same or even enhanced antitumor effects at lower doses of an individual polyphenol/drug.[4] [5]

Supercritical fluid extraction of polyphenols from plant materials seems a suitable technique for the isolation of these highly valuable, thermolabile compounds.[1] Supercritical fluid technologies have been extensively investigated for selective isolation of antioxidants from natural sources since their mild operating conditions prevent oxidation and/or degradation of labile compounds.[6] Extraction by supercritical fluids (SCFs) is not harmful to food components, it is environmentally safe and therefore represents a good alternative to other processing methods involving hazardous organic solvents and a high energy demand. The most important SCFs (SC CO2 and SC H2O) are also non-cancerogenic, non-toxic, non-flammable and thermodynamically stable.[1]

Experimental

In the recent years, the anti-carcinogenic potential of polyphenols has been intensively studied through biological processes in various cell cultures, laboratory animals and using epidemiological studies. However, not many studies have focused on how polyphenols interact with carcinogenic/toxic substances. Molecular modeling and computer simulations can provide mechanistic insight into cancer preventive actions of polyphenols without exposing oneself to carcinogenic substances.

Phenolic bioactive compound [6]-gingerol, the most abundant constituent among the gingerols in the fresh ginger rhizome, has received considerable attention as a potential therapeutic agent. The chemopreventive and chemoprotective effects exerted by [6]-gingerol are often associated with its antioxidative, antiinflammatory, antiproliferative, antiangiogenic and antiapoptotic activities.[7]

In our study, we examined [6]-gingerol from ginger as a polyphenolic scavenger of nine ultimate chemical carcinogens: aflatoxin B1 ekso-8,9-epoxide, β-propiolactone, 2-cyanoethylene oxide, ethylene oxide, chloroethylene oxide, glycidamide, propylene oxide, styrene oxide and vinyl carbamate epoxide. To evaluate [6]-gingerol efficiency, we expanded our research with the investigation of glutathione - the strongest scavenger of chemical carcinogens in human cells. Furthermore, we examined mechanisms of chemical reactions of [6]-gingerol and glutathione with the studied chemical carcinogens. Ab initio calculations of activation free energies were performed at the Hartree-Fock level of theory in conjunction with three different flexible basis sets.

According to our findings, [6]-gingerol proves to be a universal and extremely efficient natural scavenger of chemical carcinogens of the epoxy type. In comparison with glutathione, [6]-gingerol proved to be a more efficient natural scavenger of eight chemical carcinogens. The only exception was the alkylation reaction with aflatoxin B1 exo-8,9-epoxide, where [6]-gingerol and glutathione performed equally well. Moreover, the obtained results present strong evidence in favor of the validity of the proposed SN2 reaction mechanism for the alkylation reactions of [6]-gingerol and glutathione with the studied chemical carcinogens.

Our results obtained with implicit solvation methods also imply that additional protection is required for prevention of carcinogenesis triggered by the studied chemical carcinogens. Based on our results, this protection can be assured by [6]-gingerol. Moreover, the obtained results also point to the applicability of quantum chemical methods to reactions of natural scavengers with chemical carcinogens

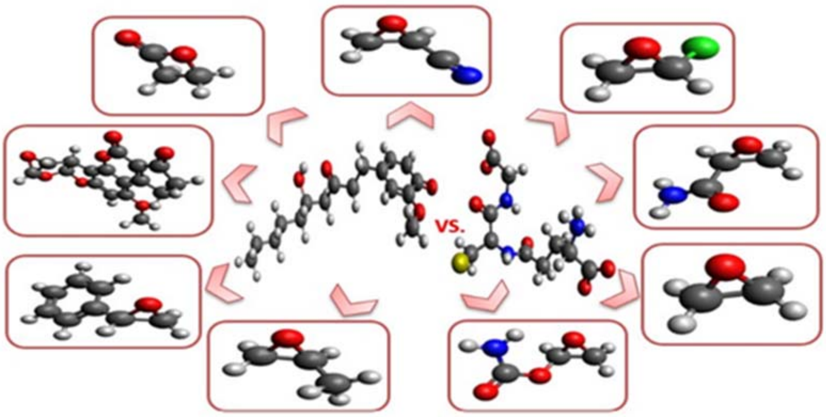

Figure 1 : [6]-gingerol versus glutathione as natural scavengers of ultimate chemical carcinogens.

Summary

We performed the first quantum mechanical evaluation of chemical interactions between two natural scavengers, namely [6]-gingerol and glutathione, and nine ultimate chemical carcinogens: aflatoxin B1 exo-8,9-epoxide, β-propiolactone, 2-cyanoethylene oxide, ethylene oxide, chloroethylene oxide, glycidamide, propylene oxide, styrene oxide and vinyl carbamate epoxide. Alkylation reactions were considered from a kinetic standpoint by assessing the ab initio calculated activation free energies and comparing them to the experimentally determined ones. With the selection of the right combination of the level of theory (Hartree−Fock), basis set (6-311++G(d,p)), and appropriate solvation model, we could obtain accurate predictions of absolute reactivity of chemical carcinogens with [6]-gingerol and glutathione.

Our quantum mechanical study of the alkylation reactions of chemical carcinogens with [6]-gingerol and glutathione provides valuable insights in the reaction mechanisms and the geometries of the transition states. Finally, the results of our study identified a novel molecular scavenger, namely [6]-gingerol, that could efficiently prevent DNA alkylation damage by covalently binding to all studied ultimate carcinogens via a lower activation barrier. Therefore, we strongly believe that our research represents the basis for further computational, experimental and clinical studies of anticarcinogenic properties of [6]-gingerol and for long-term development of novel selective dietary supplements. Moreover, the obtained results also point to the applicability of quantum chemical methods to reactions of natural scavengers with chemical carcinogens.

Acknowledgment

Financial support through Slovenian Research Agency grants J1-6736 and L7-8269 as well as through Slovenian Ministry of Education, Science and Sports program grant F4F is gratefully acknowledged. I am also grateful to Prof. Dr. Urban Bren for supervision of my research.

References

(1) Brglez Mojzer, E., Knez Hrnčič, M., Škerget, M., Knez, Ž., and Bren, U. (2016) Polyphenols: Extraction methods, antioxidative action, bioavailability and anticarcinogenic effects. *Molecules 21*, 901.

(2) Ramos, S. (2008) Cancer chemoprevention and chemotherapy: dietary polyphenols and signalling pathways. *Mol. Nutr. Food Res. 52*, 507-526.

(3) Mandžuka, Z., and Knez, Ž. (2008) Influence of temperature and pressure during PGSS™ micronization and storage time on degree of crystallinity and crystal forms of monostearate and tristearate. *J. Supercrit. Fluids 45*, 102-111.

(4) Fantini, M., Benvenuto, M., Masuelli, L., Frajese, G. V., Tresoldi, I., Modesti, A., and Bei, R. (2015) In vitro and in vivo antitumoral effects of combinations of polyphenols, or polyphenols and anticancer drugs: Perspectives on cancer treatment. *Int. J. Mol. Sci. 16*, 9236-9282.

(5) de Kok, T. M., van Breda, S. G., and Manson, M. M. (2008) Mechanisms of combined action of different chemopreventive dietary compounds. *Eur. J. Nutr. 47*, 51-59.

(6) King, M., and Bott, T. R. (1993) *Extraction of natural products using near-critical solvents*. Chapman & Hall: Glasgow, UK, 84-100.

(7) Srinivasan, K. (2017) Ginger rhizomes (Zingiber officinale): a spice with multiple health beneficial potentials. *PharmaNutrition 5*, 18-28.

Investigation of the Influence of Precursor Composition on the Characteristics of the Synthesised Activated Carbon from Lignin and Lignin-Rich Biomass

Razan Altarabeen
Institute of Thermal Separation Processes, Hamburg University of Technology, Germany.
razan.tarabeen@gmail.com

Lignin is one of the most abundant sources of organic carbon on earth, and it´s produced as a by-product of the pulp and paper industry and second generation biorefineries. Lignin has shown great potential as a precursor of various products such as cosmetics, pharmaceuticals and biopolymers, as well as activated carbons (ACs). ACs most significant features are its highly porous structure and large internal surface area (1),varying from 500 to 2000 m^2g^{-1}. which provides them with an excellent adsorptive capacity (2). Due to these properties, ACs have been frequently use as adsorbent materials in aqueous or gaseous media, and more recently in energy storage systems (e.g., electrodes or hydrogen and methane storage units). The synthesis of ACs involves two steps: 1): the precursor is thermally treated to obtain a carbon rich matrix; it can be done either by hydrothermal carbonisation or pyrolysis, and 2) chemical or physical activation of the carbon particles in order to obtain a high surface area and porosity (3).

The quality, performance, and characteristics of the synthesized ACs particles highly depend on the composition and source of the precursor as well as the thermal treatment process conditions. Some studies have identified the influence of using different sources of biomass on the behaviour of pyrolytic decomposition, e.g. when using walnut wood (hardwood), and scots pine (softwood) (4)

This work aims to investigate the influence of the lignin precursor source (e.g. type of wood: hard or soft) and the presence of polysaccharides (e.g. cellulose and/or hemicellulose) on the final characteristics of the synthesised ACs via the two above-mentioned processes. Consequently, different lignin samples obtained from Liquid Hot Water Biorefinery with varying physical properties are used as precursors for ACs.

Hydrothermal Carbonisation (HTC) is selected as a thermal treatment process as it has various advantages over the conventional pyrolysis process: it requires lower temperatures (due to exothermic reaction mechanisms), and further drying of precursor is not needed. Moreover, the impurities can be removed, and a high carbon yield is obtained (5). The reaction mechanism during HTC depends on the process conditions (e.g. temperature) and the type of biomass(6). Usually the HTC process is carried out at temperatures below 300 °C, and due to the fact that major lignin fragments are hard to /or not dissolved at these temperatures, a solid-solid reaction will take place, resulting in a polyaromatic hydrochar. This allows the lignin to retain its finely structured, strongly porous framework with the outer contours of the initial material. (7)

Chemical Activation Using KOH achieves a lower activation temperatures and shorter residence times. (5) Throughout the reaction, both chemical and physical activation are carried out allowing the formation of pore network and developing the porosity. The Metallic K is intercalated in the carbon lattice resulting in its expansion. the ACs are then washed with aqueous HCL to remove the impurities and neutralize the remaining KOH. The carbon lattices remains expanded and high porosity and surface area are obtained.

References

(1) Suhas, Carrott, P., & Ribeiro Carrott, M. (August, 2006). Lignin – from natural adsorbent to activated carbon: A review.

(2) Brun, N., A. Garcı´a-Gonza´lez, C., Smirnova, I., Titiricic, a. M., & Magdalena. (2013). Hydrothermal synthesis of highly porous carbon monoliths from carbohydrates and phloroglucinol.

(3) Rodríguez Correa, C., Stollovsky, M., Hehr, T., Rauscher, Y., & Rolli, B. (July 28, 2017). Influence of the Carbonization Process on Activated Carbon Properties from Lignin and Lignin-Rich Biomasses.

(4) Müler-Hagedorn, M., Bockhorn, H., Krebs, L., & Müller, U. (March 2003). A comparative kinetic study on the pyrolysis of three different wood species.

(5) Keat Lee, K., Hao, W., Gustafsson, M., Tai, C.-W., Morin, D., Björkman, E., Hedin, N. (2016). Tailored activated carbons for supercapacitors derived from hydrothermally carbonized sugars by chemical activation.

(6) Dinjus, Eckhard, K., andrea, T., & Nicole. (September 2011). Hydrothermal Carbonization –1. Influence of Lignin in Lignocelluloses.

(7) Kang, Shimin, L., Xianglan, F., Juan, C., & Jie. (2012). Characterization of Hydrochars Produced by Hydrothermal Carbonization of Lignin, Cellulose, D-Xylose, and Wood Meal.

Dispersion and Mass Transfer Between High Viscous Liquids and Supercritical CO_2 in a Static Mixer

Marvin Meinecke

Chair of Process Technology, Ruhr-Universität Bochum, Universitätstrasse 150, 44801 Bochum, Germany, meinecke@vtp.rub.de

Introduction

Static mixers (SM) are widely used in industries for continuous mixing of soluble substances or multiple phases [1,2]. Especially in high pressure processes, as foaming or spraying, they can be easily used as continuous mixing devices as there are no moving parts which require expensive and high-maintenance sealing. However there is small data in designing and calculating static mixers for high pressure multiphase processes. A typical two phase high pressure system is the polymer foaming process of high viscous melts with the help of physical blowing agents as CO_2 [3]. The CO_2 is added to the high viscous polymer melt while it gets distributed, dispersed and partially dissolved. However at high pressure these two main processes of dispersion and mass transfer are poorly investigated. Consequently it is the contribution of this work to study these phenomena separately. Therefore a variable high pressure plant was constructed in a first step in order to investigate the hydrodynamics and properties of a two phase system using different mixer configurations. Furthermore different observation techniques were designed allowing to investigate the simultaneously occurring effects of droplet break up and mass transfer in the static mixer. Hence there is backlight imaging for visual observations of the dispersion and background orientated schlieren (BOS) for concentration measurements. Within the scope of this work, first results of these methods will be shown.

Experimental

The experimental setup consists of three main parts: Control unit (A-C), pumping unit (D-E) and analysing unit (F-I). The system is designed in an adjustable way so that different flow modes and channels can be investigated. The control unit consists of the computer (A), pump controller (B) and heating controller (C) for data monitoring, data acquisition and flow settings. Four syringe pumps (E) heated by thermostats (D) enable the flow of three different substances. Two pumps are used for the continuous phase and another one for the dispersed phase. A third pump allows for flushing the system with a cleaning liquid. Setting the flowrate of the pumps, the substances get in contact right before they flow through the mixer (G). A high speed camera is taking pictures from the flow pattern inside the static mixer. Entering the view cell (H), the dispersion is spread into a 600 µm flat channel in order to avoid the coverage of bubbles. A second camera takes images from the view cell while a laser with a diffusor in front is used for backlight illumination. Keeping the pressure constant, a pressure retention valve (J) is installed at the end of the line.

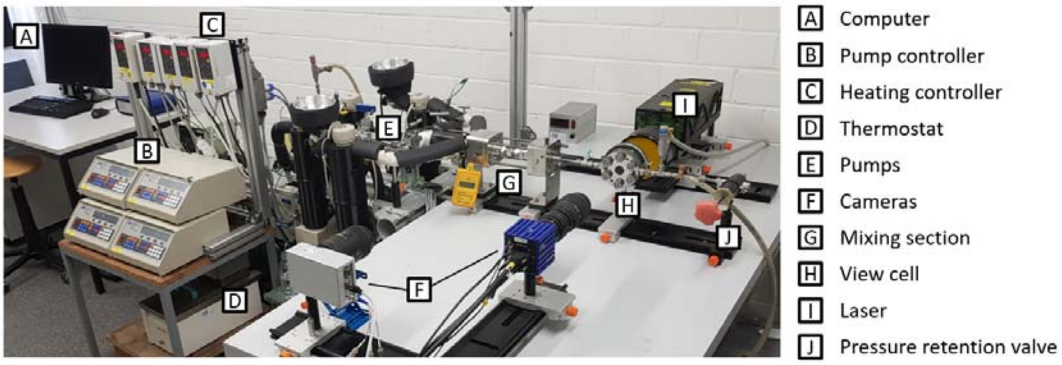

Fig. 1: Experimental set up

The images of the view cell (VC) are analysed regarding the bubble sizes and the bubble size distribution (see figure 2). Therefore an inhouse Matlab® algorithm is applied to a row of images [4]. In a first step the region of interest is cut out and gets binarised using an adjustable threshold. In order to fill all objects in a second step, a four step routine is used differentiating between several scenarios of cropped objects. Finally each white filled object is analysed regarding its shape, equivalent diameter and volume allowing to calculate the size distribution or the maximum stable bubble diameter in the flow.

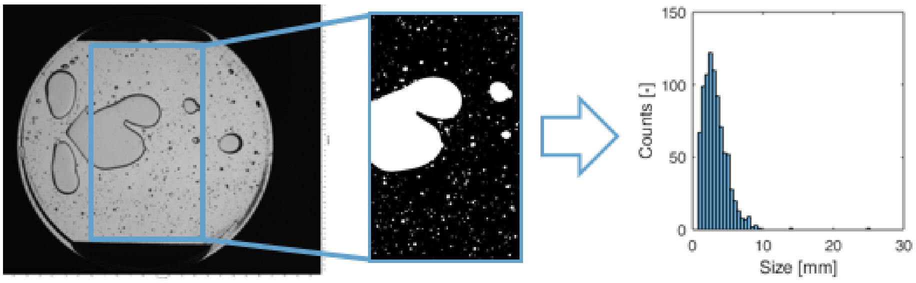

Fig. 2: Bubble detection algorithm

Measuring concentration profiles in the view cell, the camera set up slightly changes for the Background Orientated Schlieren technique (BOS). A background pattern of random distributed dots is attached to the backside of the cell, so that the camera focuses the dot pattern through the VC. Depending on the refractive index *n* of the substances inside the VC, the imaging light rays will be refracted. This leads to a change in the dot pattern in a way that some dots are shifted to new positions. Comparing the image including dot movements with an image without disturbance (constant refractive index), the shift can be obtained via multi step cross correlation. Finally the refractive index field is calculated by solving the Poisson equation applying Dirichlet and Neumann boundary conditions. [5,6]

$$\frac{\partial^2 n}{\partial x^2} + \frac{\partial^2 n}{\partial y^2} = S(x, y) \qquad (1)$$

The source term S includes the information of the shifts and the geometric dimensions of the imaging system. Calculating these shifts, an open source Matlab® application called ‘PIV lab’ is used for multi-step cross correlation [7]. A second Matlab® code is applied for processing the images including a direct solver to solve the differential equation. Finally the refractive index field is transferred into the concentration field using a previously measured calibration curve.

Testing the BOS set up, a saline solution (NaCl+H_2O) was injected over a capillary into a stream of distilled water (figure 3, left). Two images, with and without jet, were recorded and analysed. Knowing that pure water is present at the top and the bottom of the image, Dirichlet boundary conditions (BC) can be applied. However, in order to test the method all boundaries were set with Neumann BC except of Dirichlet BC at the bottom.

Consequently, the concentration is expected to start from zero at the bottom (pure water), pass a peak where the saline solution is present and fall back to the zero again.

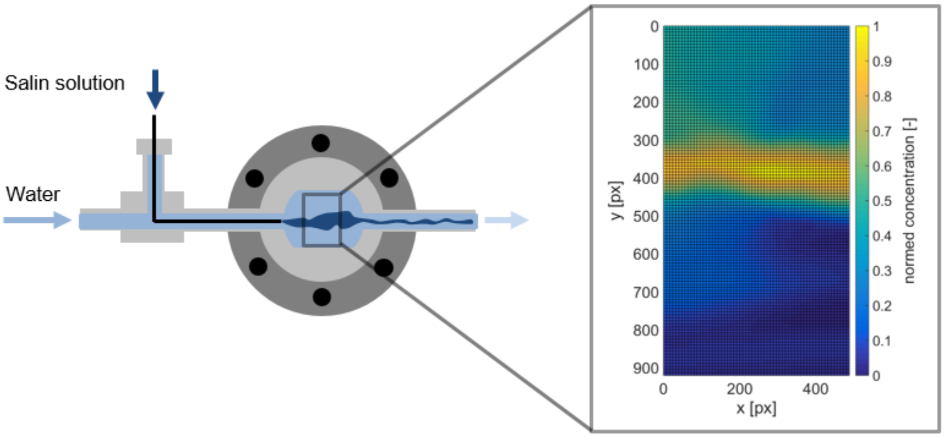

Fig. 3: BOS imaging and processing of a saline solution jet

This behaviour can be approximately seen in figure 4 on the right side proving the applicability of that method. Herein pure water is coloured in blue while the saline solution is coloured in yellow. A peak is present due to jet with a different refractive index substance, however the concentration at the top of the image is still higher than zero. This is due to the fact that the jet area is not focused by the camera and strong gradients become difficult to resolve. As a consequence errors appear while imaging and shift detection. Challenging these problems will be the task of further research.

Summary

Recording the dispersion after the static mixer via backlight imaging enable the detection of bubble sizes and bubble size distributions. The image processing is done with the Imaging Processing Toolbox^{TM} of Matlab$^{®}$. Only small changes in the set up are necessary in order to measure the concentration field in the view cell with the BOS technique. Preliminary experiments confirm the prove of concept, however further experiments are necessary to apply that method to a mixture or a two phase flow.

References

[1] R.K. Thakur, C. Vial, K. Nigam, E.B. Nauman, G. Djelveh, Static Mixers in the Process Industries-A Review, Chemical Engineering Research and Design 81 (7) (2003) 787–826.

[2] A. Ghanem, T. Lemenand, D. Della Valle, H. Peerhossaini, Static mixers: Mechanisms, applications, and characterization methods – A review, Chemical Engineering Research and Design 92 (2) (2014) 205–228.

[3] S.P. Nalawade, F. Picchioni, L. Janssen, Supercritical carbon dioxide as a green solvent for processing polymer melts: Processing aspects and applications, Progress in Polymer Science 31 (1) (2006) 19–43.

[4] MATLAB & Image Processing Toolbox, The MathWorks, Inc., Natick, Massachusetts, United States, 2016.

[5] L. Venkatakrishnan, G. Meier, Density measurements using the Background Oriented Schlieren technique, Experimental Fluids 37 (2) (2004) 237–247.

[6] M. Raffel, Background-oriented schlieren (BOS) techniques, Experimental Fluids 56 (60) (2015) 1–17.

[7] W. Thielicke, E.J. Stamhuis, PIVlab – Towards User-friendly, Affordable and Accurate Digital Particle Image Velocimetry in MATLAB, Journal of Open Research Software 2 (2014) 2–10.

Production of Pharmaceutical Dry Powders by Supercritical Assisted Coating and Co-Precipitation Processes

Ravenna Lessa Matos

Chemical Engineering Department, University of Birmingham,

RXL523@student.bham.ac.uk

Introduction

This project focuses on the use of supercritical fluids to solve two major challenges in the development of pharmaceutical powder formulations: flowability and dissolution. Supercritical fluids are attractive for particle engineering as they combine liquid-like properties (high solvation power), and gas-like properties (high diffusivity and compressibility). Supercritical fluid-based micronization is advantageous over conventional techniques since the control of particle size can be achieved via the manipulation of the operating conditions and solvent-free formulations are obtained.

In the first part of this work, the issue of poor flowability of an active pharmaceutical ingredient (API) was addressed through the combination of the supercritical antisolvent process (SAS) process with a fluidized bed under pressure (SAS-FB) to allow the simultaneous precipitation and coating of the API onto the surface of large carrier particles [1]. Curcumin has been selected as a model API and lactose as a model carrier, since it is approved as an excipient by the Food and Drug Administration (FDA) [2]. In order to improve the dissolution properties of the formulation, the coprecipitation of curcumin with a hydrophilic polymer was attempted by SAS. Polyvinylpyrrolidone (PVP) was selected as it is known to modify the crystallization kinetics of poorly water-soluble compounds by producing amorphous formulations [3].

Experimental

A schematic flowsheet of the SAS and SAS-FB processes is shown in Fig. 1. For a typical SAS-FB experiment, the conical fluidized bed is initially loaded with lactose and put inside a high pressure vessel (HPV). The HPV is pressurized with CO_2 until the desired pressure is reached and then kept at a constant flow rate. Pure solvent is delivered to the HPV through a capillary nozzle (127 µm) for 10 minutes. After this, the pump is switched to the drug solution and back to solvent to purge the pipes when the desired amount of solution has been delivered. Following this, pure CO_2 flushes the system to remove residual solvent from the formulation. Finally, the pressure is gradually decreased and the sample is collected for analysis.

In coprecipitation using the SAS process, the solution is injected from the top of the vessel and the powder is collected in a cellulose thimble (Fig. 1). The injected solution is composed of a mixture of drug and polymer in different ratios.

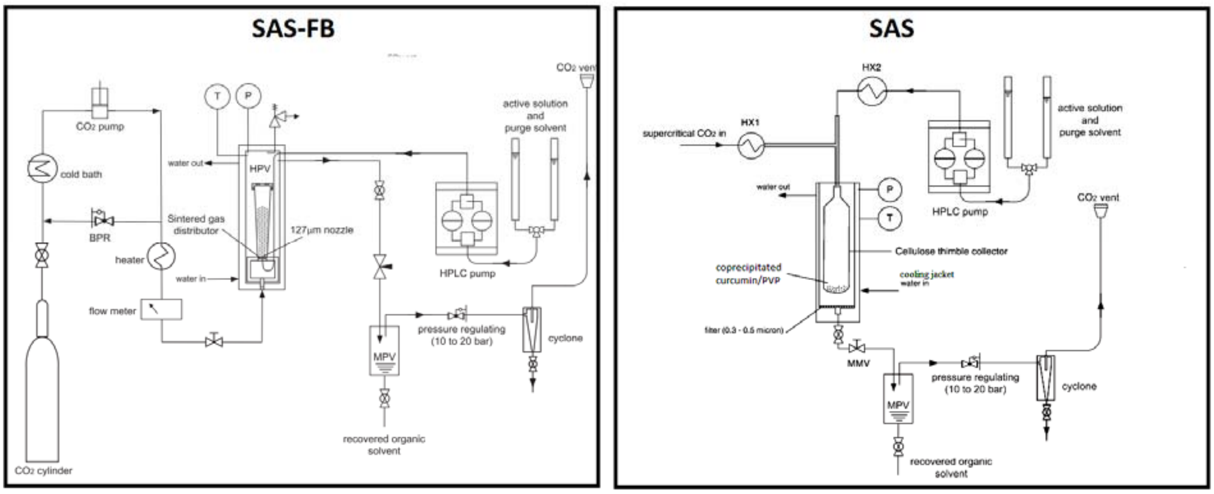

Fig. 1. SAS-FB [1] and SAS experimental apparatus. HPV = high pressure vessel, MPV = middle pressure vessel, BPR = back pressure regulator.

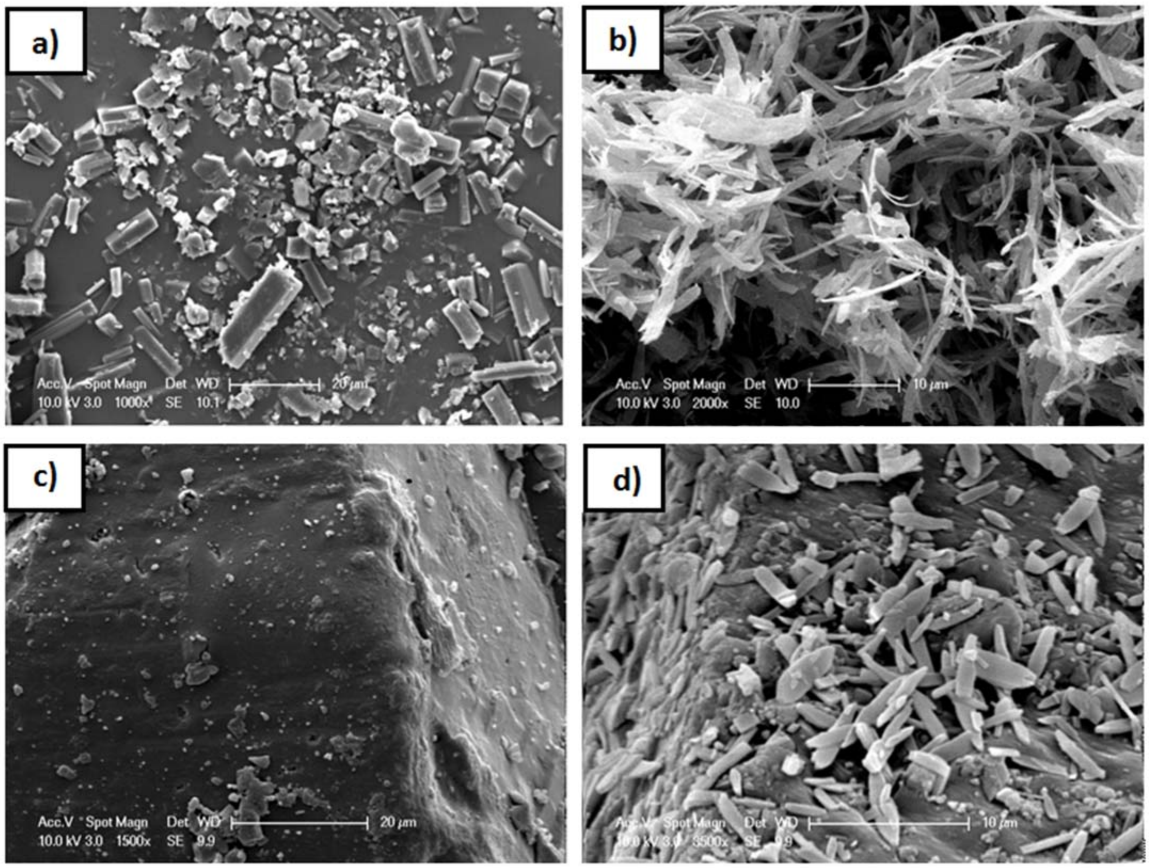

Fig. 2. a) Unprocessed curcumin; b) SAS-processed curcumin; c) unprocessed lactose; d) curcumin coated lactose by SAS-FB.

The SAS and SAS-FB experiments were carried out at 40°C, 9.0 MPa, initial solution concentration of 2 mg/ml, solution flow rate of 1 ml/min and CO_2 mass flow rate of 40 g/min. Fig. 2a shows the SEM image of unprocessed curcumin while Fig. 2b shows curcumin processed by SAS alone. A reduction in the particle size and narrowing in the particle size distribution after processing is clear; however, the high degree of particle aggregation compromises the flow properties of the formulation. SAS-FB is then used for simultaneous precipitation and coating of curcumin particles onto the surface of lactose particles (125-145 µm). Raw lactose is shown in Fig. 2c and curcumin coated lactose is shown is Fig. 2d, at a curcumin content around 2 wt%. Curcumin precipitates as individual crystals with less aggregation compared with curcumin processed by SAS alone (Fig. 2b) and with improved flow properties since it is attached to the surface of free-flowing lactose particles [2].

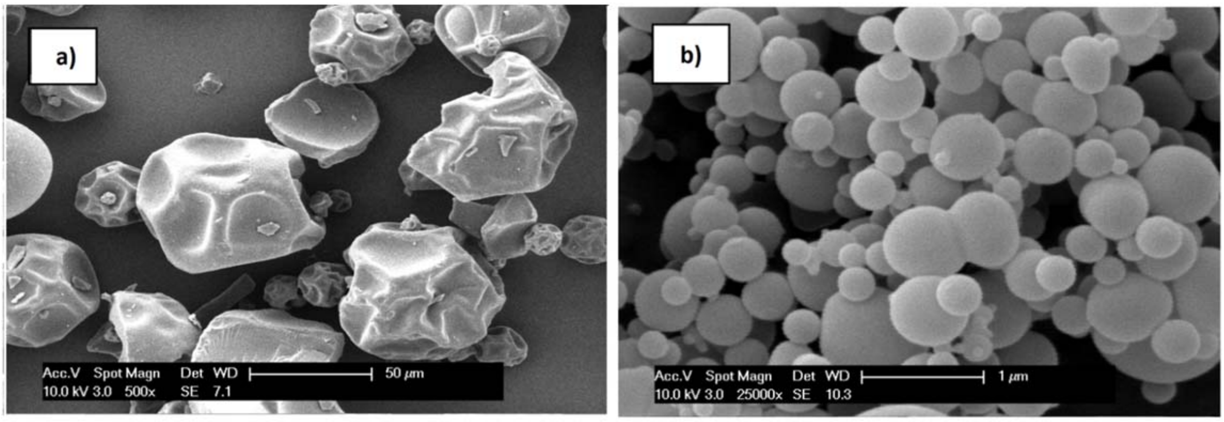

Fig. 3. a) Unprocessed PVP; b) curcumin-PVP coprecipitates processed by SAS.

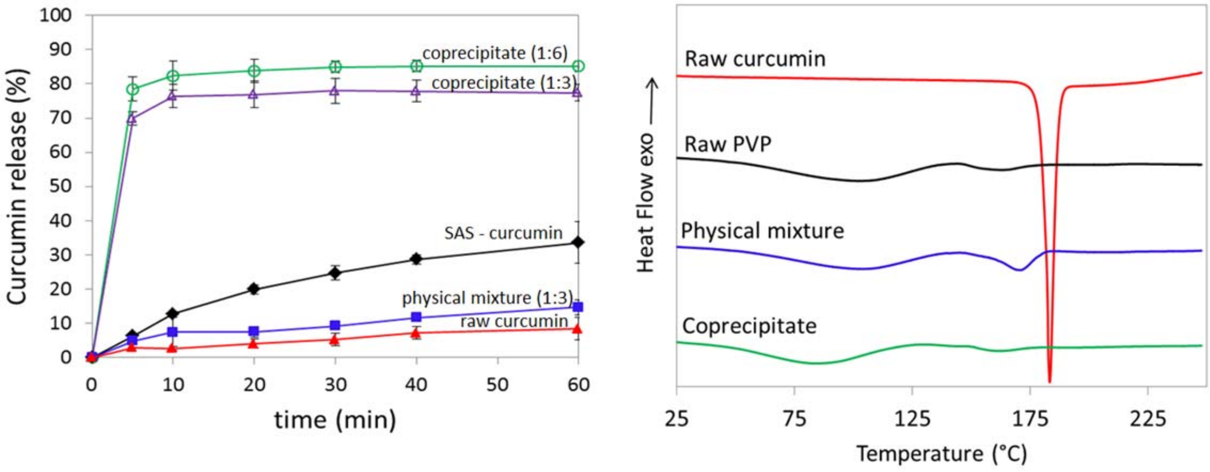

Fig. 4. a) Release test performed in water + 0.25% w/v SDS; b) DSC test.

This reduction in the particle size of curcumin was not enough to produce a significant improvement in the dissolution properties; hence the coprecipitation of curcumin with

PVP was attempted by SAS. Fig. 3a demonstrates the SEM image of unprocessed PVP, while Fig. 3b shows the result of the coprecipitation of curcumin and PVP processed at 40°C, 9.0 MPa, initial solution concentration of 10 mg/ml, solution flow rate of 0.3 ml/min, CO_2 mass flow rate of 40 g/min and 1:3 drug/polymer mass ratio. The discrete particles have improved dissolution properties as confirmed by the release test shown in Fig. 4a. This results from the formation of amorphous particles in comparison with the crystalline structure of raw curcumin as demonstrated by the Differential Scanning Calorimeter (DSC) test shown in Fig. 4b.

Summary

There are two major concerns when developing drug formulations: flowability and dissolution. In the first part of this work, the supercritical antisolvent process (SAS) was integrated with a fluidized bed under pressure (SAS-FB) to enable a simultaneous precipitation and coating of curcumin particles onto the surface of lactose particles with the aim to improve the flowability of the drug compound. In the second part, the focus is on the improvement of the dissolution properties of curcumin by the coprecipitation with a hydrophilic polymer (Polyvinylpyrrolidone).

Acknowledgment

I would like to acknowledge the financial support received from the National Council for Scientific and Technological Development (CNPQ) through the program Science Without Borders and my research team: Tiejun Lu, Valentina Prosapio, Christopher McConville, Gary Leeke and Andrew Ingram.

References

[1] Q. Li, D. Huang, T. Lu, J.P.K. Seville, L. Xing, G.A. Leeke, Supercritical fluid coating of API on excipient enhances drug release, Chem. Eng. J. 313 (2017) 317–327. doi:10.1016/j.cej.2016.12.066.

[2] R.L. Matos, T. Lu, C. McConville, G. Leeke, A. Ingram, Analysis of curcumin precipitation and coating on lactose by the integrated supercritical antisolvent-fluidized bed process, J. Supercrit. Fluids. (2017) 0–1. doi:10.1016/j.supflu.2017.12.013.

[3] V. Prosapio, I. De Marco, M. Scognamiglio, E. Reverchon, Folic acid-PVP nanostructured composite microparticles by supercritical antisolvent precipitation, Chem. Eng. J. 277 (2015) 286–294. doi:10.1016/j.cej.2015.04.149.

Degradation of PET Waste with Sub- and Supercritical Water

Maja Čolnik

Laboratory of Separation Processes and Product Design, Faculty of Chemistry and Chemical Engineering, University of Maribor, maja.colnik@um.si

Introduction

Polyethylene terephthalate (PET) is a polyester used to manufacture packaging in the food, pharmaceutical and cosmetic industries. It is one of the most commonly used plastics in the world. In the last fifty years, the use of plastic materials has grown from 5 tons per year to 100 tons per year [1]. A huge amount of generated plastic waste presents currently and, in the future, a serious environmental problem. Different decompositions processes for waste plastic were and still are under development. The PET recycling industry was created because of environmental pressures in order to improve the day-to-day management of waste. The reason for this is the very long natural decomposition of the material and the increasing use of material on a global scale.

Polyethylene terephthalate (PET) is a semi crystalline polymer derived from terephthalic acid (TPA) and ethylene glycol (EG). It has excellent tensile and impact strength, chemical resistance and appropriate thermal stability. It is hard, tough and transparent. Because of the low price it is suitable for wide use. PET has a density of 1380 kg/m^3, a melting temperature of 250 °C and a boiling temperature of 350 °C. Typical PET products are mainly foils, soft and mineral water bottles, return bottles, packing for other food-product and pharmaceuticals [1, 2]

Subcritical water is defined as water under pressure and temperature above 100 °C and below the critical point (T_c = 374 °C, p_c = 22.1 MPa). By increasing the temperature and pressure above critical point, the water passes into the supercritical area. Under subcritical and supercritical conditions, water has unique properties, as it remains in liquid state and acts as a solvent, reactant and catalyst. It has a high dissolution power. When water is exposed to sub- and supercritical conditions, major changes occur especially in polarity. An important feature of water under these conditions is the change in the ionic water product, which indicates the degree of dissociation of water into protons and hydroxyl ions [2, 3]. The use of sub- and supercritical water as a solvent does not introduce compounds that pollute the product and water is easy to remove from the degradation product [4]. Because of these properties, the sub- and supercritical water is used as an excellent media for degradation of synthetic polymers.

In this study, the effect of degradation of PET in sub- and supercritical water at different temperatures and reaction times has been investigated.

Experimental

Colorless PET bottles were used for hydrolytic depolymerization in sub- and supercritical water. The hydrolysis reaction of PET was carried out in a batch reactor at different temperatures (250, 300, 350 and 400 °C) and for reaction time from 1 to 30 min. The PET bottles were cut into small equally sized pieces, washed and dried. For each experiment the same water/PET ratio 10/1 was used. PET and water were loaded into the batch reactor that was afterwards flushed several times with N_2 to replace air. The reactor was filled with N_2 and the initial pressure was 20 bar. After that, the reactor was heated to desired temperature and then maintained at the certain temperature for selected reaction time. After desired reaction time, the reactor was immediately cooled down to room temperature, opened and the reaction product was collected.

The reaction mixture was treated with NaOH to form sodium salt of TPA (water soluble) and then acidified with concentrated HCl to precipitate TPA. The precipitated TPA was filtered, well washed with distilled water, dried, weighed and the yield of TPA was calculated. The purified TPA was confirmed by HPLC.

Summary

PET in water under sub- and supercritical conditions completely decompose to main products TPA and EG (Figure 1) [5].

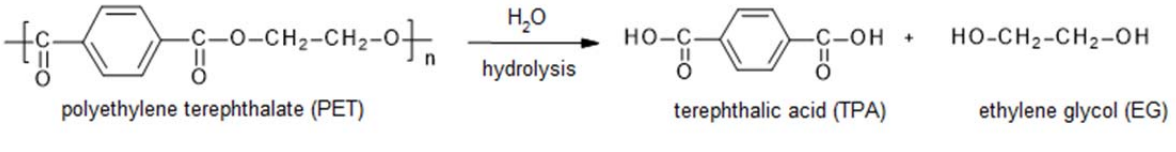

Figure 1: Depolymerization reaction of PET in water.

In our work, depolymerization of PET in sub- and supercritical water was successfully performed and the high yield of TPA was detected. In all experiments, degradation of PET was achieved completely. The highest yield of TPA was obtained in subcritical region at temperature 300 °C for reaction time 10 min and it was 95,7%. Cata et al. [5]

and Sato et al. [6] also reported about similar results, where in water at 300 °C all PET degraded and yields of TPA were 93,5% and 90%, respectively. In this study, it was found that with increasing reaction time at 250 °C, the yield of TPA increases, while at higher temperatures the yield of TPA increases to the reaction time of 10 min and then it starts to decrease, or it remains the same. Nevertheless, the PET depoymerization was completed in each case, the decrease of TPA yield was due to the formation of secondary products (benzoic acid, acetaldehyde, 1,4-dioxane and crotonic acid) [7] resulting from the degradation of terephthalic acid and ethylene glycol.

Acknowledgment

The authors would like to acknowledge the Slovenian Research Agency (ARRS) for financing this research within the frame of Programme P2-0046 (Separation Processes and Production Design).

References

[1] K. Dutta and R. K. Soni, A Review on Synthesis of Value Added Products from Polyethylene Terephthalate (PET) Waste, Polymer Science (2013) 55, 430-452.

[2] A.M. Al-Sabagh, F.Z. Yehia, Gh. Eshaq, A.M. Rabie, A.E. ElMetwally, Greener routes for recycling of polyethylene terephthalate, Egyptian Journal of Petroleum (2016) 25, 53-64.

[3] I. Pavlović, Ž. Knez, and M. Škerget, Subcritical Water – a Perspective Reaction Media for Biomass Processing to Chemicals: Study on Cellulose Conversion as a Model for Biomass, Chemical and Biochemical Engineering Quarterly (2013) 27, 73-82.

[4] X. Su, Y. Zhao, R. Zhang, J. Bi, Investigation on degradation of polyethylene to oils in supercritical water, Fuel Processing Technology (2004) 85 1249-1258.

[5] A. Căta, M. Miclău, I. Ienaşcu, D. Ursu, C. Tănasie and M. N. Ştefănuţ, Chemical recycling of polyethylene terephthalate (PET) waste using sub- and supercritical water, Revue Roumaine de Chimie (2015), 60, 579-585.

[6] O. Sato, K. Arai, M. Shirai, Hydrolysis of poly(ethylene terephthalate) and poly(ethylene 2,6-naphthalene dicarboxylate) using water at high temperature: Effect of proton on low ethylene glycol yield, Catalysis Today (2006) 111, 297-301.

[7] M. Goto, Chemical recycling of plastics using sub- and supercritical fluids, The Journal of Supercritical Fluids (2009) 47, 500-507.

Modelling of a Solution Polymerization Mini-Plant

M. Dernbach, J. Eigenseer, M. Busch*

Ernst-Berl-Institut für Technische und Makromolekulare Chemie, TU Darmstadt,
*markus.busch@pre.tu-darmstadt.de

Introduction

Within the chemical industry, the plastic segments are one of the largest sale sectors. Polyolefins hold for more than 55 % of global plastics materials demand. Among polyolefins polyethylene (PE) has the highest turnover.[1] PE is divided into different types based on its densities that are given by the structural variations. In particular, the degree and length of the branching of the backbone influences the density and material properties. A common PE type is the linear low density PE (LLDPE) with only short chain branches.[2] Its characteristic structure results from the catalytic synthesis using ethene and an α-olefin as comonomer at pressures between 10 to 200 bar and temperatures up to 300 °C. LLDPE is mainly recovered by solvent, slurry or gas phase polymerization processes.[3] In order to investigate the solution polymerization an experimental mini-plant is used. To improve the experimental procedure, a model to determine the conversion online is developed. With it, the control of the reaction can be improved and thus the experimental effort can be reduced.

Modelling

In general, the use of modelling in addition to experiments can be beneficial regarding time and costs due to reducing the necessary experimental expense. Especially in the sectors of product development and process optimization, modelling is a valuable tool. Further, it can improve the understanding of the investigated processes.

For the reactor of the LLDPE mini-plant a model for online determination of the conversion is developed based on the heat balance. The alternative gravimetrical method to determine the conversion requires several days and is therefore not suitable for an online application. The online determination allows the adjustment of the conversion during the experiments by changing the operation parameters and thus the model can reduce the experimental effort.

The heat balance for a continuous autoclave with a heating jacket consists of the heat input from the heating jacket, the heat loss to the surroundings, and the heat loss to the feed. The heat input from the heating jacket and the heat loss to the surroundings occurs through convection and conduction and is calculated using empirical correlations including the dimensionless Nusselt, Reynolds, and Prandtl numbers.[4] During the reaction, the polymerization heat is included in the heat balance whereby the amount of heat is depending on the conversion of ethene and comonomer. Further, an additional heat source is detected during the polymerization experiments at the LLDPE mini-plant. This heat source is assigned to heat produced by stirring due to experimental results in line with theoretical approaches. The amount of heat input from the stirrer depends on the composition of the solution, the synthesized polymer, and the operation parameters including pressure, temperature, and stirring speed. To reduce the complexity and number of correlations, the experimentally measured torque of the stirrer is used. The heat input of the stirrer is calibrated to the torque using experimental results. With this, the additional heat source through stirring can be calculated for further experiments.

Using the heat balance during steady state, the polymerization heat and thus the conversion can be calculated online by determining all other components of the heat balance.

Summary

For the continuous stirred tank reactor of a LLDPE mini-plant the heat balance is successfully set up and with it the conversion can be calculated online at steady state conditions. Due to estimations used in the heat balance, the accuracy of the calculated online conversion is strongly dependent on the experimental conditions during the experiments used for the calibration in comparison to the experiments, where the heat balance is applied to calculate the conversion. Within the error range, it is possible to adjust the operation parameters during experiments to obtain certain conversions.

References

[1] PlasticsEurope, **2016**, *Plastics - the Facts 2016: An analysis of European plastics production, demand and waste data*.

[2] S. Koltzenburg, M. Maskos, O. Nuyken*, Polymere – Synthese, Eigenschaften und Anwendungen*, Springer Spektrum, Heidelberg, 1. Auflage, **2014**.

[3] J. L. White, D. D. Choi, *Polyolefins – Processing, Structure Development, and Properties*, Carl Hanser Verlag, München, **2005**.

[4] VDI-Gesellschaft Verfahrenstechnik und Chemieingenieurwesen, *VDI-Wärmeatlas*, Springer Verlag, Berlin Heidelberg, 11. Auflage, **2013**.

A Transparent Micro-Device to Study Mass Transfer and Thermodynamics in Two-Phase Flows at High Pressure

Thomas Deleau
Université de Toulouse, Mines Albi, CNRS UMR 5302.
École des Mines d'Albi, Centre RAPSODEE, Campus Jarlard, 81013 Albi
Thomas.deleau@mines-albi.fr

INTRODUCTION

Concentration data and mass transfer coefficients between supercritical CO_2 and water in microfluidic capillaries are still scarce in the literature, although they are a big asset for the understanding of green chemical processes using water and supercritical CO_2.

In this study, a transparent, inexpensive and pressure resistant microsystem is developed to investigate mass transfer of a two-phase flow of water and CO_2 under high-pressure ($P > 70$ bar). It is based on microcapillary technology [1] and allows 2D axisymmetric modelling.

MATERIALS AND METHODS

2.1 Microreactor design

The microreactor developed in this study (Fig 1(a)) is based on the pressure-resistant microreactor technology developed by [1] and [2], whereby a capillary tubing is embedded in a transparent resin and supported by a polymethyl methacrylate (PMMA) chassis. In this new prototype OSTEMER resin, which has high optical quality and has shown to be resistant to pressure [2], is used for embedding the capillary tubes and ensuring optical access to the flow via a glass window.

The dimensions of the microreactor and the different elements, i.e. chassis, resin, and glass window, are shown in Fig 1(b).

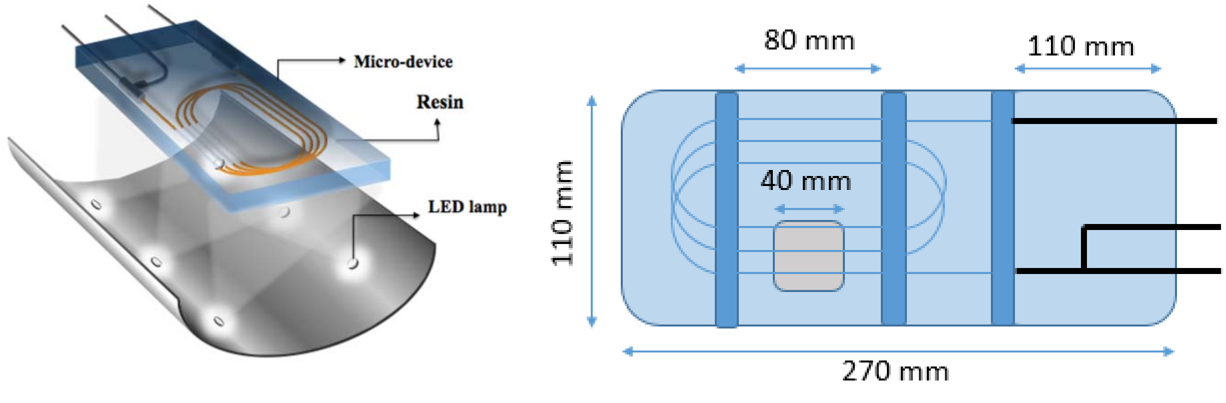

(a) (b)

Fig 1. (a) Schematic diagram of the microreactor with lighting system; (b) dimensions of the reactor with the 40mm x 40 mm viewing window and guide supports (dark blue).

2.2 Fabrication

A PMMA block (270 x 140 x 20 mm^3) is machined with a digital milling machine (Charlyrobot – Charly4U CNR3) to order to hold a glass window (40mm x 40mm) and house the coiled capillary system. A transparent box is also made in order to contain the reactor and a heating fluid. The milling process takes approximately 4 hours.

3 m of fused-silica capillary tubing (ID = 530 µm and OD = 665 µm) is coiled and inserted into the chassis and held in place with a guiding support, in which sleeves are inserted (region B in Fig 2). The plastic coating around the capillary is then carefully burned using a flame and removed with a cotton swab under a microscope in order to improve the optical transparency of the observation zone (region A in Fig 2).

OSTEMER resin (Mercene Labs) is then poured over the top of the capillary system into the PMMA/glass support, such that it entire covers the capillary tubes. The ensemble is then exposed to UV light for 35 s at 25 mW/cm^2.Crystal Clear OSTEMER resin has been chosen because of its transparency and low shrinkage properties as reported by Martin et al. [2].

Stainless-steel connectors for high pressure applications (Upchurch Scientific, USA) are used to connect the capillary reactor to the external network pipes (pumps etc.). Two phase flow is generated in the capillary using a coaxial contacting setup with a T-junction.

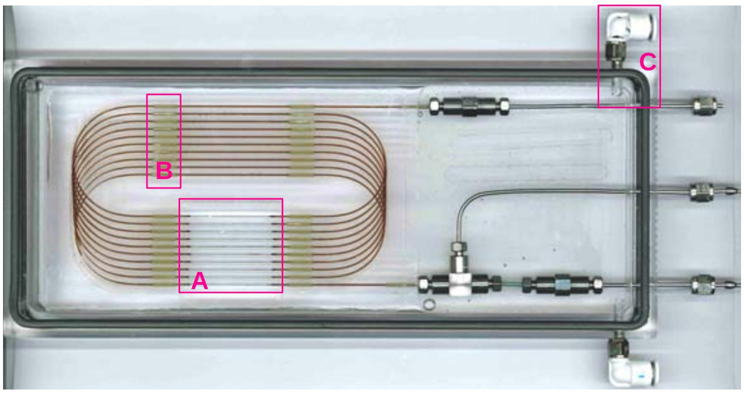

Fig 2. The transparent high pressure micro-reactor.

2.3 Experimental rig

The microreactor is integrated into a high-pressure circuit, which is fed by two syringe pumps (ISCO 260 ISCO 100 D and HLX) to reach pressures up to 20 MPa. The pumps are filled with water and with CO_2 (purity 99.995%; Linde, France), and control the volume flow rates (approximately 10^{-2} $mL.min^{-1}$) and the fluids temperature (20°C for water and 5°C for CO_2). A third syringe pump (ISCO 260 D) is placed at the outlet of the microreactor output in order to maintain and control the output pressure in the system (up to 20 MPa). The microreactor is put into a transparent box and immerged in a circulating heat transfer fluid in ordain to maintain a constant temperature in the reactor. The box has been setup to force the fluid circulation everywhere around the micro-reactor. Inlet/outlet for this heat transfer fluid is shown in Fig 2 (region C).

A Coriolis-type micro-flowmeter is used to control CO_2 mass flowrate at the microreactor inlet. Indeed, the mass flowrate is not so easy to control because of CO_2 temperature change between the pump and the microreactor inlet which involves density change. Furthermore, the pressure change affects a lot fluid properties.

Formation of the flow can be recorded by a CCD camera (Baumer HXC13) with a resolution of 1280 x 1021 pixels2. The videos can be acquired at 2000 frames per second. The microchannel is lit with LED lamps that have a light intensity of 2200 lumen. As an example, Fig 3, reports a photo of a stable two-phase Taylor flows of CO_2 and water obtained at 20 MPa using a microcapillary set-up identical to the one described in [1]. Optical access to the flow makes it possible to quantify the volume change of bubbles (due mass transfer between the gas and the liquid phases).

Fig 3. P = 20 MPa; T=308 K; V_{CO2}= 0.02 mL.min-1; V_{H2O}= 0.02 mL.min-1 in a 530 µm capillary.

The main advantage of this kind of device is the high pressure resistance, ease of fabrication and rather low price, with the “T” and “U” junctions that can be recovered after reactor failure (the lifetime of micro-reactors is not infinite due to the high pressure use).

Other advantages for hydrodynamics and mass transfer investigations lie in the circular cross section (creating an axial symmetrical system and makes CFD simulations and modelling easier), the coiling system that allows a reactor up to 10 meters long and an inner surface that is perfectly smooth.

Moreover, the cylindrical fused-silica tubing (Polymicro, USA) is coated with polyimide cladding as a protection and provides a great flexibility. When the coating is removed, the capillary is completely transparent which allows an optical access.

Finally, it should be pointed out that attention was paid to curvature effects. Indeed, curvature effects can lead to flow instabilities or to coalescence of the dispersed phase and can even be used to separate phases. For this device, the Bond number Bo = $\Delta\rho\, a_c\, L^2/\sigma$ with $a_c = v/R_{curv}$, is calculated with centrifugal acceleration. Considering identical mixtures, with identical operating conditions and with the same channel surface sections, the Bond number of the on-chip microdevices (bending radius R_{curv} = 0.3 mm) is 100 times higher than of the presented device (bending radius = 30 mm).

A few disadvantages still remain on this device: the only possible kind of entry is a coaxial one. The effect of a T-junction on high pressure can’t be investigate as carried out in Yao et al. [3]. Moreover, the current system of temperature regulation does not allow a spectroscopic access such as Raman spectroscopy some technical solutions are presently under investigations (heating film, warm air box…).

CONCLUSION AND FUTURE WORK

This work describes the fabrication of a microreactor that is able to resist pressures up to 20MPa and suitable for the use of high-pressure CO_2. The target of such a device is to use it to investigate mass transfer between gaseous CO_2 and an aqueous liquid phase. The next step of this work will consist in implementing optical techniques and/or spectroscopic techniques, which will enable concentrations of the different components to be measured along the microchannel. In combination with phenomenological modelling, this set-up will be used as a tool to calculate mass transfer coefficients between components at high pressure.

REFERENCES

[1] Macedo Portela da Silva, Nayane, Jean-Jacques Letourneau, Fabienne Espitalier, and Laurent Prat. « Transparent and Inexpensive Microfluidic Device for Two-Phase Flow Systems with High-Pressure Performance ». *Chemical Engineering & Technology* 37, n^o 11 (2014): 1929–1937.

[2] Martin Alexandre, Sébastien Teychené, Séverine Camy, et Joëlle Aubin. « Fast and Inexpensive Method for the Fabrication of Transparent Pressure-Resistant Microfluidic Chips ». Microfluidics and Nanofluidics 20, no 6 (1 juin 2016): 92.

[3] Yao, Chaoqun, Zhengya Dong, Yuchao Zhao, et Guangwen Chen. « The Effect of System Pressure on Gas-Liquid Slug Flow in a Microchannel ». AIChE Journal 60, no 3 (1 mars 2014): 1132-42.

Conversion of CO_2 Capture by Ammonia into Value-Added Chemicals

Juan I. del Río, A. Martín, M.D. Bermejo

High Pressure Processes Group, Department of Chemical Engineering and Environmental Technology, Universidad de Valladolid (Spain)

riverignacio@gmail.com

Introduction

The concentration of greenhouse gases, mainly CO_2 particularly from burning fossil fuels, has increased the global concerns about climate change [1]. The Paris Agreement has the objective of limiting global warming to no more than 2°C above the temperature in pre-industrial times by reducing CO_2 emissions [2]. To achieve it, the European Union, and the rest of the international community, encourage the use of renewable energies, but it can be foreseen that for many years it will still be necessary to use fossil fuels for the production of electricity and as fuel in the automotive industry [3, 4]. Therefore, other solutions are considered, such as CO_2 capture and storage technologies (CCS) [5], which would significantly reduce the CO_2 emissions of thermal plants and chemical industries such as the production of ammonia, hydrogen, steel and cement [6].

Among the processes of CO_2 capture, the use of amine solutions is the most developed today, although it still has important limitations such as the high cost of desorption. Recently the French company Alston developed a technology known as “Chilled Ammonia”, based on a similar principle [7]. Instead of using an amine aqueous solution, combustion gases are absorbed into an ammonia aqueous solution (28%wt) at low temperature (2-10ºC), to absorb CO_2 as carbonate, bicarbonates and carbamates of ammonia. As in the case of amines, regeneration is produced by desorption at temperatures between 100-150ºC at pressures between 3 and 136 bar. This process has the advantage that the heat of absorption is much lower than in the case of amines, its regeneration is cheaper economically and energetically, but it presents the disadvantage of using a lot of cooling.

Fossil-oil resources are also the main source of raw materials for the synthesis chemical industry. Hence, in the long term, the CO_2 conversion technologies can provide a substitute source of these basic chemical compounds. In this matter, several green chemistry technologies have been able to yield value-added chemicals from hydrogenating CO_2 derived ammonium carbamate/carbonate [9]. However, the use of gaseous hydrogen suppose the a non-sustainable fossil fuel based economy, which can be overcome through environmentally friendly and economical hydrogen production technologies like Aluminum-water splitting (following the equation: $2Al+6H_2O \rightarrow 2Al(OH)_3 + 3H_2$), getting advantage of the water present in the aqueous amine solutions. The use of reducing metals such as zinc and aluminum, or biomass derivatives, have proven to be effective in reducing sodium bicarbonate in hydrothermal media with efficiencies of up to 60% [1]. In the case of CO_2 dissolved by amines as carbamates, it is known that its reactivity is greater than that of bicarbonate [9]. On the other hand, aqueous solutions of amines and ammonia are able to absorb much higher amounts of CO_2 than that dissolved as bicarbonate. The objective of this work is to revalorize CO_2 by replacing the desorption given in conventional processes with a stage of catalytic conversion in a hydrothermal media to value-added products (e.g. formic acid), without separation, purification or compression processes.

Experimental

Ammonium Carbamate (AC) (99%), was used as CO_2 source, in a 0,5 M aqueous solution, using water class II. Pd powder (<1µm, >=99.9%) and Pd/C (5wt% loading) were used as catalysts. Aluminum fine powder (Al) (<5µm, 99.5%) was employed as reducing metal. All reagents, except aluminum (Panreac), were purchased from Aldrich. All chemicals were used without further purification.

The reactions were carried out in a 25mL Parr reactor with stirring (500 rpm) (Fig 1.), at 120ºC during 2h. The Al:AC molar ration was kept at 6:1, and 0.1g of Pd/catalysts and 0.005g Pd powder were added according to the experimental design. The air inside the reactor, containing the Al, was flushed with nitrogen during 20 min before heating to 120ºC. During the heating ramp, the reaction solution was pumped in order to avoid the carbamate decomposition, as well as undesired premature releasing of hydrogen, and to allow a better temperature control at the set point. The reaction products were analyzed by HPLC using an Aminex 87H (Bio-Rad) column.

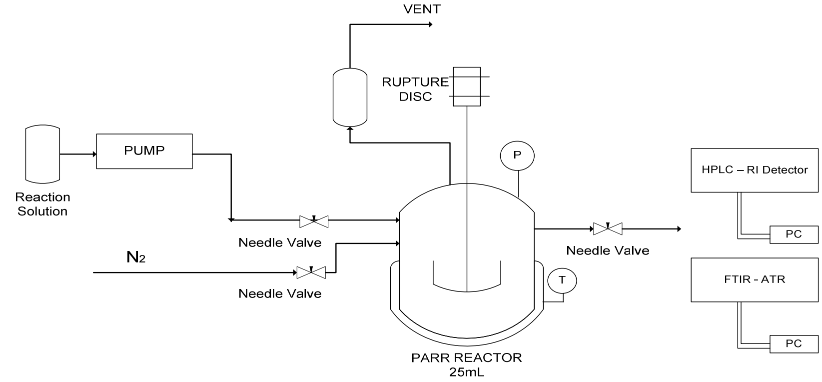

Fig. 1. Reducing reaction system.

Results

Fig 2 shows the yield of formic acid and bicarbonate with and without catalysts. The positive effect of Pd/C on the formic yield (12%) is clearly noted as the Al+Pd powder reaction showed a similar performance than the control reaction (only Al), suggesting that this reaction requires the addition of catalyst. This can be attributed to the characteristic dispersion of active sites of the Pd/C commercial catalyst of about 23.2% in the carbon surface area [9], also indicating that this kind of support doesn't have a deleterious effect in the reaction. The bicarbonate yield is the lowest in Al+Pd/C reaction, suggesting a lower presence of decomposition products of the carbamate (according to the equation: $NH_3 + CO_2 + H_2O \rightarrow NH_4HCO_3$). When using Pd/C catalyst, the autogenic pressure rise to 4.8 bar, the lowest pressure among the tested conditions, and may be due to a higher adsorption of hydrogen in the catalyst, increasing its availability for the reduction reaction, along with a less release of decomposition products (NH_3 and CO_2).

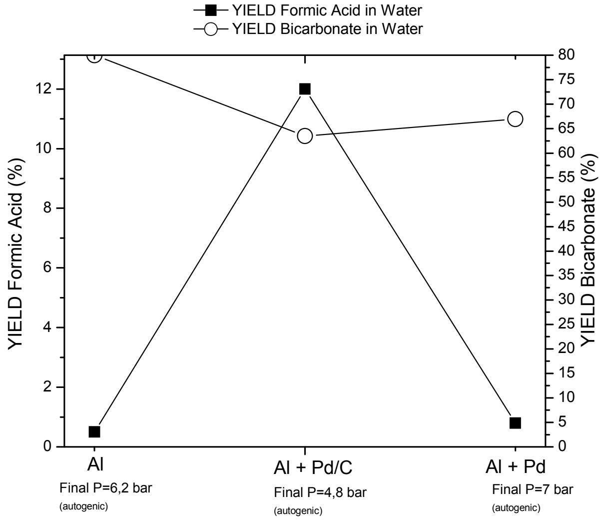

Fig. 2. Product yields in the hydrothermal reduction of AC with and without catalysts.

Summary

The experiments presented show that it is possible to obtain formic acid (FA) from hydrothermal reduction of CO_2 derived ammonium carbamate at 120ºC, with areaction tiem of 2 h, using Al as reductor and Pd/C as catalyst, without gaseous H_2, with a yield of formic acid higher than 10%. Ethanol solutions also showed an increase of formic yield when using Pd/C catalyst, which will be part of the future work in order to pursue higher yields. The methodology proposed allowed lowering the reaction temperature with respect to hydrothermal reduction of CO_2 as bicarbonate, what would allow to minimize energy consumption in hydrothermal process. Moreover, scarce works have been found in the hydrothermal reduction of carbamates for producing value-added chemicals, representing a promising field of innovation.

Acknowledgment

Authors thank the Spanish Ministry of Economy and Competitiveness for the project ENE2014-53459-R. M.D. Bermejo thanks the Spanish Ministry of Economy and Competitiveness for a Ramón y Cajal fellowship.

References

[1] M. Pérez-Fortes, E. Tzimas, Techno-economic and environmental evaluation of CO2 utilisation for fuel production, JRC Science Hub: ZG Petten, The Netherlands, (2016).

[2] J. Rogelj, M. Den Elzen, N. Höhne, T. Fransen, H. Fekete, H. Winkler, R. Schaeffer, F. Sha, K. Riahi, M. Meinshausen, Paris Agreement climate proposals need a boost to keep warming well below 2 C, Nature, 534 (2016) 631.

[3] E.J. Maginn, What to Do with CO2, ACS Publications, 2010.

[4] P. Styring, E.A. Quadrelli, K. Armstrong, Carbon dioxide utilisation: closing the carbon cycle, Elsevier2014.

[5] H. Yang, Z. Xu, M. Fan, R. Gupta, R.B. Slimane, A.E. Bland, I. Wright, Progress in carbon dioxide separation and capture: A review, Journal of environmental sciences, 20 (2008) 14-27.

[6] B. Llamas, B. Navarrete, F. Vega, E. Rodriguez, L.F. Mazadiego, Á. Cámara, P. Otero, Greenhouse Gas Emissions–Carbon Capture, Storage and Utilisation, Greenhouse Gases, InTech2016.

[7] E. Gal 2006. Ultra cleaning combustion gas including the removal of CO2. World Intellectual Property, Patent WO 2006022885. (2006)

[9] J. Su, M. Lu, H. Lin, High yield production of formate by hydrogenating CO 2 derived ammonium carbamate/carbonate at room temperature, Green Chemistry, 17 (2015) 2769-2773.

Analysis of Limonene Filled Yeast Cell Microcapsules

Cornelia Errenst

Institute of Thermo- and Fluiddynamics/ Department of Mechanical Engineering,
Ruhr-University Bochum, errenst@vtp.rub.de

Introduction

Yeast cells are deployed in the production of beer, bioethanol and in the baking industry. Within these processes, spent yeast cells occur as by-product and are then sold as animal feed or used for the yeast extract production. In the production of yeast extracts, spent brewer’s and baker’s yeast cells are emptied through an autolysis. During the autolysis components from the inside of the cells, like part of the cytoplasm, proteins, part of RNA and DNA, are broken down using enzymes and extracted under specified conditions. The produced yeast extract is sold i.a. as flavour enhancer and sandwich spread. The remaining emptied yeast cells, so called ghost cells, are sold as animal feed for around 2€ per kilogram.

But ghost cells still contain lots of valuable components like proteins, polysaccharides and β-glucans. Therefore, they could also be processed in food for human consumption. Moreover, after autolysis the yeast cell wall is still intact. This is one of the reasons for ghost cells being a promising material for the encapsulation of oils, flavours, active agents and dyes. It is possible to encapsulate photosensitive, odorous, easy oxidizable or volatile substances inside the yeast cells to protect them against uv-radiation, oxygen and higher temperatures. [1]

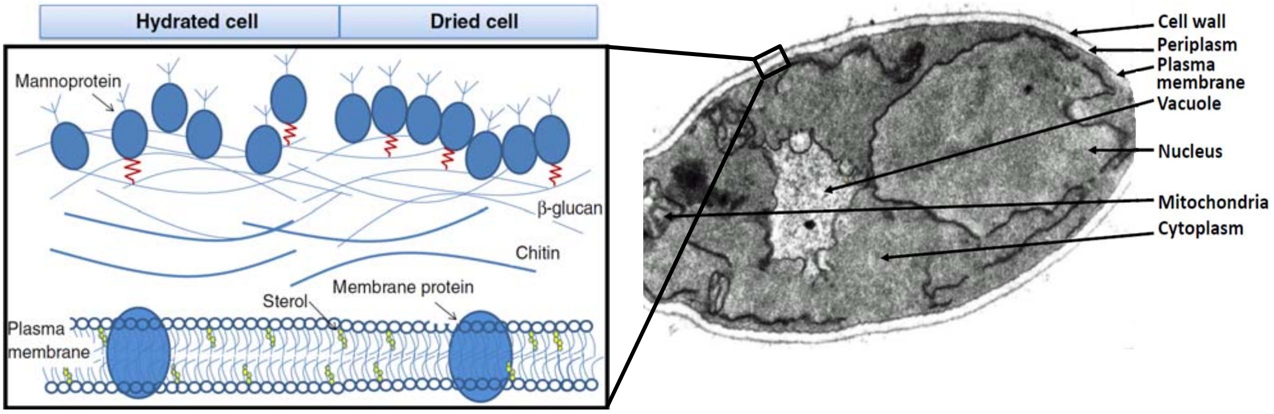

Fig. 1: Scheme of a hydrated and a dried yeast cell wall (left) and a picture of a yeast cell labelling all components (right). [2]

When the cell wall is hydrated, the comprised mannoproteins work like a sieve with a mesh size depending on their water content. Molecules, depending on their molecular weight, viscosity and solubility in the yeast cell plasma membrane, can diffuse through the cell wall into the ghost cell. When the cell wall is dry, the molecules are trapped inside and diffusion in both directions is stopped. The scheme in Fig. 1 (left) explains the position of the mannoproteins in hydrated and dried yeast cells. [2] [3]

Encapsulation is carried out by mixing yeast cells, water and the substances to be encapsulated for 1 to 24 hours at 40 to 60 °C. Afterwards the yeast cells are washed and spray or freeze dried. The produced microcapsules find use in a wide range of applications, for example for flavours in food products or washing agents, for active substances in medicine or animal feed, additives in composite materials or biocides in agricultural industry. [1] [2]

Experimental

The focus of this work is on the analysis of yeast microcapsules filled with limonene, as a model substance, in order to verify that the limonene molecules are trapped inside the yeast cells and not only adsorbed at the surface. To determine the total limonene content of the microcapsules, they were first moistened with water to facilitate diffusion and thereafter extracted with ethanol. The limonene concentration of the extract was analysed using gas chromatography/ mass spectrometry (GC/ MS). To determine the amount of limonene which is situated around the yeast cell and adsorbed at the surface, the microcapsules were washed using a Soxhlet extractor. Therefore, the cells were weighed into an extraction thimble and extracted for 20 h using hexane as solvent. Subsequent the hexane was analysed to get the amount of limonene on the surface of the cells.

In addition, the washed microcapsules were dried, moistened with water and extracted again with ethanol to analyse the total limonene content after the removal of the surface limonene. Fig. 1 (right) shows the analysis of the total limonene content of microcapsules before the Soxhlet extraction, the analysed surface limonene content and the limonene content of the cells after they were washed with hexane. Through the fact that there were just 0.37 wt.-% of limonene washed off the microcapsules and that there were still 25.35 wt.-% limonene analysed after the washing, it could be shown that the limonene was encapsulated inside the yeast cells.

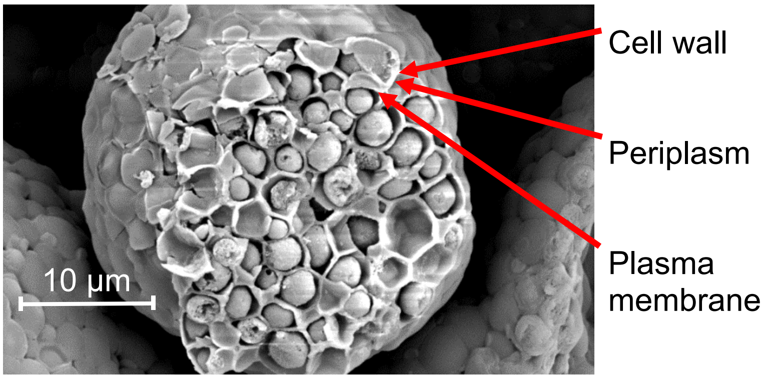

Total limonene content [wt.-%]	25.61
Surface limonene content [wt.-%]	0.37
Total limonene content after Soxhlet [wt.-%]	25.35

Fig. 2: Scanning electron microscope picture of an broken agglomerate of hundreds of yeast cell microcapsules (left) and analysis data of these microcapsules before and after Soxhlet extraction (right)

Another possibility to verify that limonene is trapped inside the yeast is using thermogravimetric analysis (TGA). In the course of these measurements the microcapsules are heated up to temperatures higher than the boiling point of limonene (which is 175 °C) while the mass is weighed. In doing so, it can be shown that there is no mass loss in this temperature range, which means that no limonene escaped from the inside of the yeast cells. Normand et al. showed that yeast cells are thermostable up to temperatures of around 250 °C till they start breaking [4].

Within this work TGA measurements were done heating the microcapsules up from 25 to 400 °C with a heating rate of 5 k/min. It was shown that no mass loss occurred between temperatures of 175 to 210 °C. This means that the yeast cells were thermostable up to temperatures of 210 °C until breaking and releasing of limonene starts. One possibility for the significant difference to the 250 °C, identified by Normand et al., could be the difference in the heating rate. Normand et al. chose a fast heating rate of 20 K/min whereas in this study a heating rate of 5 K/min was set [4]. In further TGA measurements at varied heating rates should be examined if there is a dependency of the heating rate on the breaking of the cells.

To get information about how the yeast cell microcapsules look like, scanning electron microscope (SEM)-pictures were prepared. Fig. 1 (left) shows a SEM picture of agglomerates of microcapsules with a limonene content of around 25 wt.-%. Due to the damage of the microcapsules it is possible to see the cell wall, the plasma membrane and the periplasm between these layers.

Summary

In this study it could be verified that limonene was encapsulated inside yeast cells and not only adsorbed at the outer surface using two different approaches. On the one hand the limonene content was analysed before and after washing the microcapsules with hexane using a Soxhlet extractor. In addition, TGA measurements were done to prove that no limonene escaped from the yeast cells although the sample is heated up to higher temperatures than the boiling point of limonene.

References

[1] Paramera EI, Karathanos VT, Konteles SJ (2014) Yeast Cells and Yeast-Based Materials for Microencapsulation. In: Microencapsulation in the food industry: A practical implementation. Elsevier Academic Press, S.l., pp 267–281

[2] Pham-Hoang BN, Romero-Guido C, Phan-Thi H et al. (2013) Encapsulation in a natural, preformed, multi-component and complex capsule: yeast cells. Appl Microbiol Biotechnol 97(15): 6635–6645. doi: 10.1007/s00253-013-5044-1

[3] Dardelle G, Normand V, Steenhoudt M et al. (2007) Flavour-encapsulation and flavour-release performances of a commercial yeast-based delivery system. Food Hydrocolloids 21(5-6): 953–960. doi: 10.1016/j.foodhyd.2006.12.013

[4] Normand V, Dardelle G, Bouguerand P et al. (2005) Flavor Encapsulation in Yeasts: Limonene Used as a Model System for Characterization of the Release Mechanism. Journal of Agricultural and Food Chemistry

Preparation and Analysis of Polar Hawthorn Berry Extracts, Industrial Application in Poultry Processing Procedure

Márta Kubovics[1], Said Al-Hamimi[2], György Huszár[3], Charlotta Turner[2], Edit Székely[1]

kubomarti@gmail.com

[1]Department of Chemical and Environmental Process Engineering, Budapest University of Technology and Economics, Hungary
[2]Centre for Analysis and Synthesis, Department of Chemistry, Lund University, Sweden
[3]Taravis Ltd., Sárvár

Introduction

Hawthorn (*Crataegus* sp.) is a traditional herb with well-known positive effects to the cardiovascular system, commonly used to prevent and treat several heart diseases, such as congestive heart failure, high blood pressure, hyperlipidemia, cardiac arrhythmia. [1] The pharmacological effects are attributed to the polyphenol content of the herb: phenolic acids, flavonoids, procyanidin oligomers and anthocyanins have been observed in the berries, flowers and leaves of the plant. [2,3]

We propose, that the benefical cardiovascular effects can be utilized in the livestock raising industrial sector as well. In the poultry processing industry, it is an actuality for years, that due to the shortened rearing time, the capillaries of the animals are not strong enough. According to regulations, during the processing procedure chickens are stunned using electrical shock before cutting. Due to the electric shock, the not fully-fledged capillaries snap off in the chicken breast, and blood spots appear inside the meat. These spots have to be removed before selling due to the need of the market, causing huge economical loss, since the value of the produced ”cut off meat” is low compared to the chicken breast fillet.

Our aims are to show that the cardiovascular development of the animals can be positively influenced by feeding chickens with a tincture containing hawthorn extract. Therefore the extent of the blood spots and the amount of the low-value meat can be decreased. The analysis of the polar extract, namely the determination of the total polyphenol, tannin, flavonoid content, the antioxidant efficiency and identification of the main phenolic compounds were also performed.

Experimental

Preparation of the drinking tincture

Hawthorn was air-dried in an attic and was grinded (particle size: 1 mm). Pilot scale supercritical CO_2 extraction was carried out to reduce the oily and fatty components of the plant (extractor: 450 bar, 50 °C, separators: 40, 20 bar) in order to avoid any emulsion formation in the further conventional extraction step with a polar solvent. Brunner-equation was fitted to the experimental data (Fig. 1). Nearly the maximal yield (2.5%) was achieved with 14 kg CO_2/kg dry material (appr. after 180 minutes).

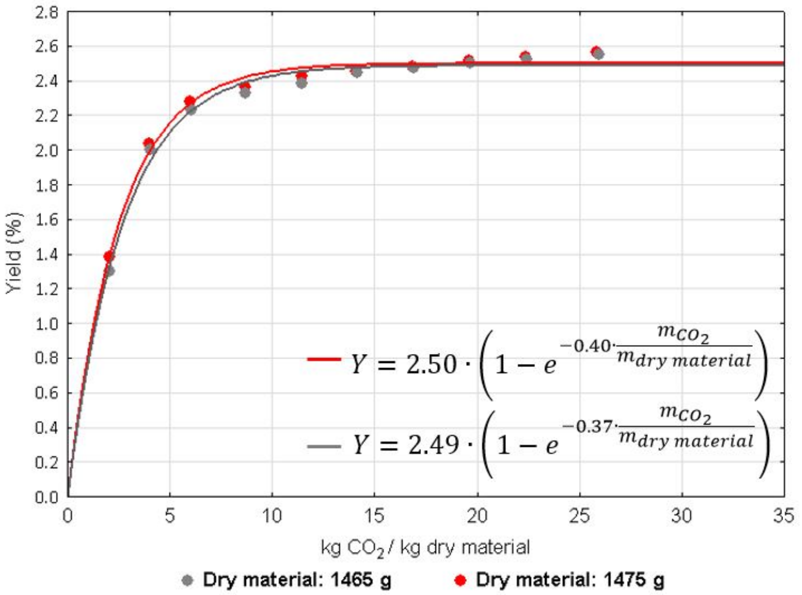

Figure 1 Extraction curves of hawthorn berries obtained with supercritical fluid extraction

The extraction residue of the berries was processed with pilot scale Soxhlet extraction using ethanol (96%) (extractor temp.: 50 °C) to obtain a polar extract enriched in phenolic compounds (yield: 25.9± 3.0% on dry basis). As a result of the extraction a concentrate was produced (appr. 2.1 liter), containing ethanol (66.3 m/m%). In the last step this concentrate was dissolved in tap water (10 v/v%) and acidifying material (LUPRO-CID; 0,098 v/v%)) was added to avoid infection of the animals. To obtain a pure tincture, the solution was centrifuged (1500 1/min, 5 min) and the supernatant was diluted 10 times volume (appr. 1 v/v% dry extract; less, than 0.7 m/m% ethanol) for the chickens in the poultry farm.

Analytical investigation

Total polyphenol and tannin content were determined by the Folin-Ciocalteu method [4]. Radical scavaging activity was evaluated by the DPPH method, while for the flavonoids, the their abitily to form yellow complex with aluminium were used. [5] The main phenolic compounds were identified using ultra-high performance liquid chromatography coupled to quadrupole time-of-flight mass spectrometry in both positive and negative ESI modes.

Regarding the total composition of the plant material, (Table 1) a comparison can be made with previous publications. The polyphenol content of the plant is slightly lower, than in the cited paper (0.83% vs 1.28%), the tendency is reversed in case of the tannins (0.19% vs 0.10%). [6] The low flavonoid content is reasonable, since those are the most abundant components of the leaves, not the berries. [2] The antioxidant efficiency of the Soxhlet extract (compared at IC_{50} values, 55.00±1.82 µg/ml) is appr. 3 times weaker compared to BHT reference (18.71±1.67 µg/ml), since the lower IC_{50} concentration means higher radical scavaging activity.

Table 1: Total bioactive contents of hawthorn extract and the plant, using pyrogallol and quercetin equivalent as reference (PE%, QE%: g reference equivalent/100 g extract)

Total bioactive compound contents		
	Pilot-scale Soxhlet extract	Plant material
Phenolic content (PE%)	3.220±0.031	0.834±0.008
Tannin content (PE%)	0.736±0.047	0.191±0.012
Flavonoid content (QE%)	0.100±0.004	0.026±0.001

The identification of the main phenolic compounds were peformed on the basis of previously reported compounds in plants. Several phenolic acids (caffeoylquinic acid isomers), procyanidins (dimer, trimer, tetramer forms, epi(catechin) and glycolised dimer) and flavonoids in glycolised form (quercetin 3-O-hexoside, cratenacin isomer, rutin and isorhamnetin O-hexoside) were obsreved.

Drinking experiment

100 chickens were randomly separated from the stock, as an experimental group and 100 non-treated chickens were used as control group. The two groups were reared and processed in the same way, except for the feeding: for one week the experimental group was fed with the hawthorn drink, the control group drank water with the same concentration of the acidifying agent. A comparison between the groups was made regarding the extent of the blood spots in the chicken breast –appearing during the procession- first visually, and then, on the basis of the quantity of the removed low value meat.

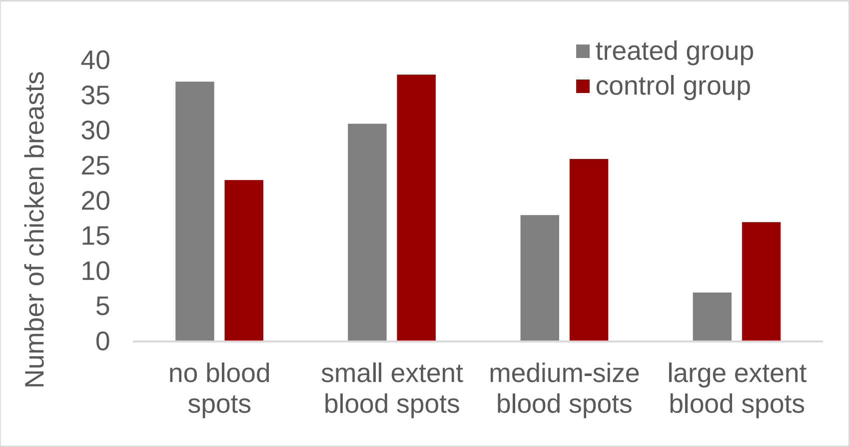

Figure 2 Number of chicken breasts classified visually in four roughly defined groups

The meats were classified in four roughly defined groups. (Fig. 2) Noticeable improvement was achieved regarding the size of the blood spots. The number of chicken breasts without blood spots increased by 50% as well. Logistic regression showed, that at significance level of 0.05 the size of the blood spots decreased (p=0.004). Regarding the quantities of low quality cut off a huge improvement was achieved, in case of the treated group 7.74% of the full meat weight was removed, while in the control group this value was 21.39%. It is important to note that the weights of the chicken breasts in the treated group slightly lower compared to the control group. This might be the effect of the treatment, however these lower weights are still in the optimal range. Moreover the distribution of the weights are tighter in the treated group, which is a preference in the technology.

Summary

The hawthorn berries can induce positive effects to the cardiovascular system of the chickens. To prepare a suitable alcoholic extract the removal of the apolar fraction with supercritical fluid extraction is advantageous as the foaming is reduced. The amount of the polyphenols and tannins are roughly correspond to already reported values, however flavonoid content is low, and the antioxidant efficiency is much weaker than the reference's. By analysing the main compounds, several phenolic acids, procyanidins and flavonoids were detected.

A treatment of the developing chickens with a drinking tincture made from hawthorn berries can decrease the extent of blood spots, appearing during the processing procedure inside the chicken breast. However the decreasing weight of the meat needs to be taken into consideration. The preparation procedure of the tincture, and total phenolic compound determination were also performed.

Acknowledgment

The method for the analysis was developed and the investigation was performed in Green Technology Group of Lund University, Sweden, where M.K. spent nine weeks financed by the Erasmus+ programme of the EU. The drinking test was performed in the poultry farm of Hegyháti Broiler Kft, Hungary. Extraction experiments were performed and evaluated at BME. This work was supported by the Higher Education Excellence Program of the Ministry of Human Capacities in the frame of Biotechnology research area of Budapest University of Technology and Economics (BME FIKP-BIO).

References

[1] Chang, W.T., Dao J., Shao, Z., " Hawthorn: Potential Roles in Cardiovascular Disease" The American Journal of Chinese Medicine, 33, pp. 1-10, 2015

[2] Yang, B., Liu, P., "Composition and health effects of phenolic compounds in hawthorn (Crataegus spp.) of different origins" Journal of the Science of Food and Agriculture, 92, pp. 1578–1590, 2012

[3] Nabavi, S. F., Habtemariam, S., Ahmed, T., Sureda, A., Daglia, M., Sobarzo-Sánchez, E., Nabavi, S. M., "Polyphenolic Composition of Crataegus monogyna Jacq.: From Chemistry to Medical Applications", Nutrients, 7, pp. 7708–7728, 2015

[4] Magyar Gyógyszerkönyv, “Pharmacopoea Hungarica”, VIII. edition. 2.8.14. Article, pp. 232, Medicina Könyvkiadó Rt., Budapest, 2003-2010

[5] Höltzlné Plánder, Sz.: Gyógynövénykivonatok antioxidáns hatásának jellemzése, “Characterizing the antioxidant efficiency of herbs”, Budapest University of Technology and Economics, Department of Chemical and Environmental Process Engineering, 2015

[6] Froehlicher, T., Hennebelle, T., Martin-Nizard, F., Cleenewerck, P., Hilbert, J., Trotin, F., Grec, S. "Phenolic profiles and antioxidative effects of hawthorn cell suspensions, fresh fruits, and medicinal dried parts" Journal of Food Chemistry, 115, pp. 897-903, 2009

Experimental and Simulation-Based Study of Decomposition Processes with Regard to the LDPE High-Pressure Synthesis

Anton Hilfer, Markus Busch*

Department of Chemical Engineering and Macromolecular Science,

Technische Universität Darmstadt, anton.hilfer@pre.tu-darmstadt.de,

*markus.busch@pre.tu-darmstadt.de

A major challenge in high-pressure synthesis of LDPE are spontaneously occurring decompositions. From a thermodynamic point of view, ethene is relatively unstable. The process parameters of the high-pressure polyethylene synthesis are close to a pressure and temperature limit where a decomposition with the main products carbon black, methane and hydrogen can occur.[1] Decompositions are the result of an exceedance of a critical temperature limit due to a hot spot in the process. Typical causes that lead to a hotspot, are incorrect or poorly adjusted control of inlet-flows and temperatures, mechanical on the bearing of the stirrer, impurities in the feed or inhomogeneities due to poor mixing.

As a result, in a decomposition temperature and pressure rise up to a maximum of 1500 °C and 4500 bar. Since high-pressure polymerization plants are not designed for such drastic conditions, there is a great interest in describing the decomposition process and its limits comprehensively to be able to minimize risks by means of better process control and plant design in order to avoid damages and expensive downtimes.

There have been many studies dealing with ethene decompositions with the focus on the determination of stability limits, the decomposition behavior and the optimal process management. With the work of Watanabe[3] and Zhang et al.[2], a first kinetic approach of the decomposition reaction of ethene was established. Subsequent publications, dealing with the modeling of decomposition processes, are based on the kinetics proposed by Watanabe and Zhang. However, one important relation has not been considered in previous works yet. In ignition experiments have shown that behavior of decomposition varies widely, depending on the position of the ignition point. This can only be explained by means of the flow properties within the autoclave. In order to observe the flow conditions during decomposition, a new experimental setup is necessary.

In this work, the decomposition process of ethene is investigated in a view-cell autoclave. As a result, it is possible to capture the flame front during the decomposition process, and extract the propagation speed in dependence of pressure and temperature. Based on this, spatially- and time resolved *Computational Fluid Dynamics* (CFD) simulations are performed to aquire insight of the relationship between the flow properties and the decomposition reaction of ethene.

To find a suitable approach for the simulation model, current research from the modeling conventional combustion systems are investigated and correlated with the measured flame velocities. Results are, that the decomposition of ethene can be described as a premixed combustion. The modeling of a premixed combustion is a very challenging task, since it occurs as a thin, spreading flame front which is stretched and distorted by turbulences. To resolve the flame front, the internal flame structure, detailed chemical kinetics and molecular diffusion processes need to be calculated in a spatially resolved manner. This makes a direct kinetic modeling almost impossible due to the high requirements for resolution of the computational grid, in particular if the transient behavior of a flame is to be investigated. Therefore, this work uses a combustion model, which permits the simulation of the propagation of the flame front with relatively low computational effort. The advantage of such a combustion model is the decoupling of chemistry and kinetics from flow properties and flame front behavior. For this purpose, the combustion chamber is subdivided into a burned and unburned area which is characterized by the transport of a scalar which describes the propagation of the flame front. To consider combustion products and reaction species, a tabulated kinetic (flamelet library approach) is implemented in the simulation model. In summary, the established CFD simulation model enables the modeling of ethene decomposition reactions in relation to the flame front propagation and the reacting species.

References

[1] T. Zimmermann, G. Luft, *Chemie Ingenieur Technik* **1994**, 66, 1386-1389.

[2] S. X. Zhang, N. K. Read and W. H. Ray, *Aiche Journal* **1996**, 42, 2911-2925.

[3] H. K. H. Watanabe, M. Takehisa, *PACHEC* **1972**.

Registered Lecturers

Prof. Zeljko Knez	University of Maribor, Slovenia zeljko.knez@uni-mb.si
Prof. Urban Bren	University of Maribor, Slovenia urban.bren@um.si
Dr. Amra Perva-Uzunalic	University of Maribor, Slovenia amra.uzunalic@um.si
Dr. Masa Knez-Hrncic	University of Maribor, Slovenia masa.knez@um.si
Ao.Prof. Thomas Gamse	Graz University of Technology, Austria Thomas.Gamse@TUGraz.at
Dr. Eduard Lack	Natex Prozesstechnologie, Austria office@natex.at
Dr. Helena Sovova	Institute of Chemical Process Fundamentals, Czech Republic, sovova@icpf.cas.cz
Prof. Marcus Petermann	Ruhr University Bochum, Germany petermann@fvt.ruhr-uni-bochum.de
Prof. Markus Busch	Technical University Darmstadt, Germany markus.busch@pre.tu-darmstadt.de
Prof. Eberhard Schlücker	University Erlangen Nürnberg, Germany sl@ipat.uni-erlangen.de
Dr. Carsten Zetzl	Hamburg University of Technology, Germany zetzl@tuhh.de
Dr. Pavel Gurikov	Hamburg University of Technology, Germany pavel.gurikov@tuhh.de
Prof. Maria Jose Cocero	University of Valladolid, Spain mjcocero@iq.uva.es
Prof. Angel Martin Martinez	University of Valladolid, Spain mamaan@iq.uva.es
Prof. Jacques Fages	Ecole des Mines d'Albi, France Jacques.Fages@mines-albi.fr

Prof. Edit Szekely	Budapest University of Technology and Economics, Hungary, sz-edit@mail.bme.hu
Prof. Irena Zizovik	Wroclaw University of Science and Technology, Poland irena.zizovic@pwr.edu.pl
Prof. Carl Schaschke	Abertay University, United Kingdom c.schaschke@abertay.ac.uk
Prof. Charlotta Turner	Lund University, Sweden charlotta.turner@chem.lu.se
Prof. Can Erkey	KOC University Istanbul cerkey@ku.edu.tr

Registered Participants

Martin Rozman	SI	University of Maribor
Maja Čolnik	SI	University of Maribor
Veronika Furlan	SI	University of Maribor
Vincent Bürk	DE	Ruhr University Bochum
Marvin Meinecke	DE	Ruhr University Bochum
Cornelia Errenst	DE	Ruhr University Bochum
Michael Feist	DE	Universität Erlangen-Nürnberg
Maria Dernbach	DE	Technical University Darmstadt
Christoph Mohl	DE	Technical University Darmstadt
Anton Hilfer	DE	Technical University Darmstadt
Razan Taraben	DE	Hamburg University of Technology
Alberto Bueno Moralez	DE	Hamburg University of Technology
Juan del Rio	ES	University of Valladolid
Thomas Deleau	FR	Ecole des Mines d’Albi
Marta Kubovics	HU	Budapest University of Technology and Economics
Surika van Wyk	NL	University of Twente
Fiona Nermark	SE	Lund University
Ravenna Lessa Matos	UK	University of Brimingham